Supplemental material to this article can be found at:
http://jpet.aspetjournals.org/content/suppl/2020/10/30/jpet.120.000258.DC1

1521-0103/376/1/106–117$35.00
THE JOURNAL OF PHARMACOLOGY AND EXPERIMENTAL THERAPEUTICS
Copyright © 2020 by The American Society for Pharmacology and Experimental Therapeutics
https://doi.org/10.1124/jpet.120.000258
J Pharmacol Exp Ther 376:106–117, January 2021

The Journal of PHARMACOLOGY And Experimental Therapeutics

Inhibiting Sialidase-Induced TGF-β1 Activation Attenuates Pulmonary Fibrosis in Mice[S]

Tejas R. Karhadkar, Thomas D. Meek, and Richard H. Gomer

Departments of Biology (T.R.K., R.H.G.) and Biochemistry and Biophysics (T.D.M.), Texas A&M University, College Station, Texas

Received July 30, 2020; accepted October 6, 2020

ABSTRACT

The active form of transforming growth factor-β1 (TGF-β1) plays a key role in potentiating fibrosis. TGF-β1 is sequestered in an inactive state by a latency-associated glycopeptide (LAP). Sialidases (also called neuraminidases (NEU)) cleave terminal sialic acids from glycoconjugates. The sialidase NEU3 is upregulated in fibrosis, and mice lacking Neu3 show attenuated bleomycin-induced increases in active TGF-β1 in the lungs and attenuated pulmonary fibrosis. Here we observe that recombinant human NEU3 upregulates active human TGF-β1 by releasing active TGF-β1 from its latent inactive form by desialylating LAP. Based on the proposed mechanism of action of NEU3, we hypothesized that compounds with a ring structure resembling picolinic acid might be transition state analogs and thus possible NEU3 inhibitors. Some compounds in this class showed nanomolar IC_{50} for recombinant human NEU3 releasing active human TGF-β1 from the latent inactive form. The compounds given as daily 0.1–1-mg/kg injections starting at day 10 strongly attenuated lung inflammation, lung TGF-β1 upregulation, and pulmonary fibrosis at day 21 in a mouse bleomycin model of pulmonary fibrosis. These results suggest that NEU3 participates in fibrosis by desialylating LAP and releasing TGF-β1 and that the new class of NEU3 inhibitors are potential therapeutics for fibrosis.

SIGNIFICANCE STATEMENT

The extracellular sialidase NEU3 appears to be a key driver of pulmonary fibrosis. The significance of this report is that 1) we show the mechanism (NEU3 desialylates the latency-associated glycopeptide protein that keeps the profibrotic cytokine transforming growth factor-β1 (TGF-β1) in an inactive state, causing active TGF-β1 release), 2) we then use the predicted NEU3 mechanism to identify nM IC_{50} NEU3 inhibitors, and 3) these new NEU3 inhibitors are potent therapeutics in a mouse model of pulmonary fibrosis.

Introduction

Fibrosis involves scar-like tissue forming in an internal organ leading to organ failure (Martinez et al., 2017). Pulmonary fibrosis has an incidence of 1 in 400 in the elderly, and there are no Food and Drug Administration–approved therapeutics that stop the progression of this disease (Raghu et al., 2011; Wynn and Ramalingam, 2012; Raghu and Selman, 2015). Transforming growth factor-β1 (TGF-β1) in its active mature form is a key factor that potentiates fibrosis (Fernandez and Eickelberg, 2012; Wolters et al., 2014). TGF-β1 is synthesized as a precursor protein made of latency-associated peptide (LAP) and the active TGF-β1 in a complex called latent TGF-β1 (L-TGF-β1) (Hinck et al., 2016; Robertson and Rifkin, 2016). Two dimerized TGF-β1 precursor proteins are processed to cleave active TGF-β1 from the LAP, with the LAP remaining essentially wrapped around and sequestering the TGF-β1 (Robertson and Rifkin, 2016). Like many other secreted proteins, LAP is glycosylated (Lewandrowski et al., 2006; Moremen et al., 2012; Travis and Sheppard, 2014; Hinck et al., 2016; Robertson and Rifkin, 2016).

Several things can release active TGF-β1 from sequestration by the LAP. Both the integrin αvβ6, which generates mechanical traction on the LAP, and thrombospondin-1 can release active TGF-β1 (Crawford et al., 1998; Munger et al., 1999). Proteases, such as plasmin, thrombin, matrix metalloproteinase-2, and matrix metalloproteinase-9, and reactive oxygen species–mediated conformational changes in LAP, can also release TGF-β1 from the LAP (Lyons et al., 1988; Pociask et al., 2004; Jobling et al., 2006; Jenkins, 2008) However, it is unclear whether these are the only mechanisms that cause upregulation of active TGF-β1 in fibrotic lesions.

Neuraminic acid (also known as sialic acid) is a sugar found at the terminal ends of some glycoproteins (Varki and Gagneux, 2012; Schwab and Nimmerjahn, 2013; Varki et al., 2015). The presence or absence of sialic acid on these glycoconjugates has

This work was supported by National Institutes of Health National Heart, Lung, and Blood Institute [Grant R01 HL132919]. T.R.K., T.D.M., and R.H.G. are inventors on a patent application for the use of this class of sialidase inhibitors as therapeutics for a variety of diseases.
https://doi.org/10.1124/jpet.120.000258.
[S] This article has supplemental material available at jpet.aspetjournals.org.

ABBREVIATIONS: AMPCA, 4-amino-1-methyl-2-piperidinecarboxylic acid; 2AP, 2 acetylpyridine; BAL, bronchoalveolar lavage; brhNEU3, bacterially expressed recombinant human NEU3; B SA, bovine serum albumin; DANA, 2,3-didehydro-2-deoxy-*N*-acetyl-neuraminic acid; HEK293, human embryonic kidney 293; IL-6, interleukin-6; LAP, latency-associated glycopeptide; L-TGF-β1, latent TGF-β1; MBP, maltose-binding protein; MP, methyl picolinate; 4MU-NANA, 2′-(4-methylumbelliferyl)-α-D-*N*-acetylneuraminic acid sodium salt hydrat; NEU, neuraminidasee; OCI, oxacarbenium ion intermediate; PBMC, peripheral blood mononuclear cell; rhLAP, recombinant human LAP; rhL-TGF-β1, recombinant human L-TGF-β1; rhNEU, recombinant human NEU; TGF-β1, transforming growth factor-β1.

Downloaded from jpet.aspetjournals.org at ASPET Journals on April 19, 2024

a central role in various cellular regulatory mechanisms (Varki and Varki, 2007; Zhou et al., 2020). For instance, adding sialic acids to the glycan residues on IgG confers anti-inflammatory functions to IgG (Anthony and Ravetch, 2010). Conversely, the loss of sialic acid from the plasma glycoprotein serum amyloid P attenuates the potency of serum amyloid P to inhibit the differentiation of some human peripheral blood mononuclear cells (PBMCs) to fibrosis-associated fibroblast-like cells called fibrocytes (Cox et al., 2015).

Neuraminidases (also known as sialidases) are enzymes that catalyze a hydrolysis reaction that removes terminal sialic acids from glycoconjugates (Miyagi et al., 2012; Pshezhetsky and Ashmarina, 2013; Smutova et al., 2014). There are four known mammalian sialidases (Miyagi et al., 2012; Smutova et al., 2014). Of the four, the sialidase NEU3 is localized in endosomal structures and on the extracellular side of the plasma membrane and under some conditions can also be released by cells, and thus it can desialylate glycoproteins and glycolipids present outside the cell (Kopitz et al., 2001; Zanchetti et al., 2007; Miyagi and Yamaguchi, 2012; Mozzi et al., 2015; Rodriguez-Walker and Daniotti, 2017). Sialidases, especially NEU3, are upregulated in pulmonary fibrosis (Lambré et al., 1988; Karhadkar et al., 2017; van de Vlekkert et al., 2019). TGF-β1 upregulates NEU3 in human lung epithelial cells, pulmonary fibroblasts, small airway epithelial cells, and PBMCs (Karhadkar et al., 2017). In the epithelial cells, TGF-β1 increases levels of NEU3 by decreasing the NEU3 degradation rate and increasing *NEU3* mRNA translation (Chen et al., 2020). Conversely, NEU3 upregulates TGF-β1 in human PBMCs and human pulmonary fibroblasts (Karhadkar et al., 2017). Intratracheal delivery of bleomycin upregulates TGF-β1 in the lungs (Cutroneo et al., 2007; Yue et al., 2010), and is a standard model of pulmonary fibrosis in mice (Moore et al., 2013; Blackwell et al., 2014). Mice lacking NEU3 or wild-type mice treated with sialidase inhibitors do not upregulate TGF-β1 in the lungs after bleomycin treatment and show attenuated bleomycin-induced pulmonary fibrosis (Karhadkar et al., 2017, 2020). Together, these observations suggested that a positive feedback loop in which TGF-β1 upregulates NEU3 and NEU3 upregulates TGF-β1 may potentiate fibrosis (Karhadkar et al., 2017, 2020). How NEU3 upregulates TGF-β1 is unknown.

Bacterial and viral sialidases can desialylate L-TGF-β1, leading to the release of active mature TGF-β1, possibly explaining why there are elevated levels of active TGF-β1 levels during infection with sialidase-expressing pathogens (Miyazono and Heldin, 1989; Miyazono et al., 1991; Schultz-Cherry and Hinshaw, 1996; Carlson et al., 2010; Gratz et al., 2017). There have been many previous attempts to develop inhibitors for viral (von Itzstein, 2007) or human (Cairo, 2014) sialidases. Examples of viral sialidase inhibitors include Tamiflu (oseltamivir) and Relenza (zanamivir), which can attenuate the progression of influenza in patients (Hayden et al., 1997; Monto et al., 1999; Mäkelä et al., 2000; Moscona, 2005). Potent inhibitors for viral neuraminidases exert poor inhibition for human neuraminidases (Hata et al., 2008; Albohy et al., 2011). There are a variety of inhibitors for human sialidases, but all have published IC_{50} of ~10 μM for NEU3, making them relatively weak inhibitors (Potier et al., 1979; Magesh et al., 2006; Albohy et al., 2010; Zou et al., 2010; Cairo, 2014; Guo et al., 2018).

In this report, we find that NEU3 desialylates LAP to release active TGF-β1. We then identified a new class of potent NEU3 inhibitors, some with IC_{50} in the nM range. These compounds inhibit bleomycin-induced pulmonary fibrosis in mice, further supporting the idea that NEU3 inhibitors may be potential therapeutics for fibrosis.

Materials and Methods

Cell Isolation and Culture. Human peripheral blood was collected from healthy volunteers who gave written consent with specific approval from the Texas A&M University human subjects review board. All methods were performed in accordance with the relevant guidelines and regulations. Blood collection, isolation of PBMCs, and cell culture were done as described previously (Pilling et al., 2009a,b).

Mouse NEU3 Expression in Human Embryonic Kidney 293 (HEK293) Freestyle Cells. HEK293 freestyle cells (Life Technologies, Grand Island, NY) were cultured in FreeStyle 293 media (12338-018; Life Technologies). Cells (1×10^5) were mixed with 2 μg of 100 μg/ml of murine Neu3 expression clone (MR223297; Origene, Rockville, MD) in 100 μl PBS (GE Lifesciences, Marlborough, MA) and were transfected by electroporation using a 4D-Nucleofector System (Lonza, Walkersville, MD) following the manufacturer's protocol. The transfected cells were kept at room temperature for 15 minutes for recovery, after which the cells were cultured in 25 ml Freestyle 293 media in a humidified incubator at 37°C with 5% CO_2. After 24 hours, 400 μg/ml of G418 (345812; Calbiochem EMD, San Diego, CA) was added to select for transfected cells. After 10 days, the cells were isolated and lysed, and c-Myc–tagged recombinant mouse NEU3 was purified using a Myc-Trap_A kit (ytak-20; Chromotek, Hauppauge, NY) following the manufacturer's protocol. The eluted protein was stored in 50 μl of 10% glycerol, 100 mM glycine, and 25 mM Tris-HCl, pH 7.3, at 4°C.

Human NEU3 Expression in *Escherichia Coli*. The human NEU3 cDNA sequence was amplified from a human NEU3 open reading frame clone (RC216537; Origene). The amplified NEU3 sequence was inserted between the NdeI and *EcoR*I sites of the pMAL-c5X vector (N8108S; NEB, Ipswich, MA). The resulting construct encoding a fusion of maltose-binding protein (MBP) and NEU3 was transformed into chemically competent E. cloni cells (Lucigen, Middleton, WI) mixed in 37°C prewarmed LB broth (240230; BD, Franklin Lakes, NJ); grown with shaking at 37°C, 240 rpm for 1 hour; and plated on LB agar with ampicillin (100 μg/ml). Clones were selected and grown in 100 μg/ml ampicillin LB broth medium, and the plasmids were isolated using a GeneJET Plasmid Miniprep Kit (K0502; Thermo Scientific, Waltham, MA). Clones were verified by sequencing (Eton Bioscience, San Diego, CA). The sequence-verified clones were transformed into chemically competent BL21(DE3) *E. coli* cells (Lucigen); grown with shaking at 37°C, 240 rpm, for 1 hour in prewarmed LB broth; and plated on LB agar with 100 μg/ml ampicillin. Individual colonies were selected and added to 10 ml prewarmed LB broth with 100 μg/ml ampicillin and grown at 37°C, 240 rpm, for no longer than 16 hours. The culture was added to 1 l of LB broth and incubated at 37°C, 240 rpm, until (optical density measured at wavelength 600 nanometers) OD_{600} = ~0.6. To induce protein expression, isopropyl β- d-1-thiogalactopyranoside (Goldbio, St. Louis, MO) solution was added to 0.5 mM and incubated at 20°C at 240 rpm overnight. Protein purification was done as described previously (Albohy et al., 2010) with the following modifications. Bacterial cells were harvested after 16–18 hours of induction by centrifugation at 4000*g* at 4°C. The pellet was resuspended in resuspension buffer (20 mM Tris, pH 7.2; 300 mM NaCl; 1 mM EDTA; and 0.1% Triton X-100) supplemented with 1× protease inhibitor (PIA32965; VWR, Radnor, PA). The lysate was sonicated three times for 3 minutes with the tube submerged in ice at setting 16 of a Microson ultrasonic cell disruptor (Misonix Incorporated, Farmingdale, NY) and then clarified by centrifugation at 10,000*g* for 20 minutes at 4°C. The supernatant was loaded onto an amylose column (New England

Downloaded from jpet.aspetjournals.org at ASPET Journals on April 19, 2024

Biolabs) equilibrated with 20 mM Tris/300 mM NaCl, pH 7.2. MBP-NEU3 was eluted with running buffer containing 10% glycerol (v/v) and 20 mM maltose.

Sialidase Effects on LAP Assay. To determine the effect of sialidases on LAP, 400 ng/ml human recombinant LAP (246-LP/CF; R&D Systems, Minneapolis, MN) was incubated with and without 200 ng/ml of human recombinant sialidases NEU1 (TP300386; Origene), NEU2 (TP319858; Origene), NEU3 (TP316537; Origene), or NEU4 (TP303948; Origene) or *Clostridium perfringens* neuraminidase (N2876-2.5UN; Sigma-Aldrich, St. Louis, MO) in a total volume of 20 μl of 1× PBS (SH30256.01; GE Lifesciences), pH 6.9. The PBS was adjusted to pH 6.9 with 12N HCl (H613-05; Avantor Performance Materials, Radnor Township, PA). The reaction mixtures were incubated at 37°C for 2 hours. After incubation, 5 μl of 4× Laemmli's buffer (GTX16355; GeneTex, Irvine, CA) containing 20 mM dithiothreitol was added to the reaction mixtures, and these were heated at 100°C for 5 minutes. Fifteen microliters of the heated reaction mixture was electrophorized on a 4–20% Tris/glycine polyacrylamide precast gel (12001-058; VWR) in Tris/glycine/SDS running buffer (13.5 g Tris base, 7.2 g glycine, 5 g SDS/l) at room temperature for 90–120 minutes.

Western blots and staining the blots with lectin were done as previously described (Cox et al., 2015), and immunostaining Western blots for NEU3 was done as previously described (Karhadkar et al., 2017, 2020). Silver staining of gels was done following (Morrissey, 1981). Staining intensity was quantified by Image Laboratory software (Bio Rad, Hercules, CA).

NEU3 Induced L-TGF-β1 Activation Assay. To determine whether NEU3 can cause L-TGF-β1 to release active TGF-β1, 200 ng/ml recombinant human L-TGF-β1 (299-LT/CF; R&D Systems) was incubated with varying concentrations of sialidases with or without 1 mM calcium chloride in a total volume of 100 μl of PBS, pH 6.9, in a 96-well microplate. The microplates were covered with aluminum foil and incubated at 37°C for 2 hours. After incubation, the reaction mixtures were assayed using an active TGF-β1 ELISA kit (DY240; R&D Systems) following the manufacturer's protocol with the exception that the reaction mixtures were not processed for acid treatment so as to measure only active TGF-β1 and not total TGF-β1. The absorbance was read with a SynergyMX plate reader (BioTek, Winooski, VT). To determine the enzyme kinetics of NEU3 with L-TGF-β1 as a substrate, varying concentrations of L-TGF-β1 were incubated with 100 ng/ml of recombinant human NEU3 (Origene) in a total volume of 100 μl, and the samples were processed as described above.

Sialidase Activity Assay with 2′-(4-Methylumbelliferyl)-α-D-*N*-acetylneuraminic Acid Sodium Salt Hydrate. Sialidase assays were done following Potier et al. (1979) and Marathe et al. (2013) with the following modifications. PBS was adjusted to pH 6.9 with 12N HCl, and bovine serum albumin (BSA) (VWR) was added to a final concentration of 100 μg/ml (PBS-BSA). Varying concentrations of bacterially expressed recombinant human NEU3 were prepared in PBS-BSA. A final concentration of 200 μM 2′-(4-methylumbelliferyl)-α-D-*N*-acetylneuraminic acid sodium salt hydrate (4MU-NANA) (M8639; Sigma-Aldrich) was added to the NEU3 in a total volume of 100 μl in a 96-well plate. When indicated, inhibitors were added for 30 minutes before adding the 4MU-NANA. The reactions were incubated at 37°C for 30 minutes, and the fluorescence was measured at 37°C in a prewarmed SynergyMX plate reader with excitation at 360 nm and emission at 440 nm. The fluorescence in the absence of sialidases was subtracted from all readings.

Inhibition of NEU3 Induced L-TGF-β1 Activation. 2,3-didehydro-2-deoxy-*N*-acetyl-neuraminic acid (DANA) (252926-10MG) was purchased from EMD-Millipore (Burlington, MA), Oseltamivir phosphate (Tamiflu) was purchased from (1479304) Sigma, 2-acetylpyridine (2AP) (sc-254121) was purchased from Santa Cruz Biotechnology (Dallas, TX), and methyl picolinate (MP) (sc-228575) was purchased from Santa Cruz. 4-Amino-1-methyl-2-piperidinecarboxylic acid (AMPCA) (A00285-13785-026) was synthesized by Sundia (Shanghai, China) following the scheme shown in Supplemental Fig. 1. These compounds were dissolved in water to 20 mM. All stocks were stored at 4°C and used within 2 weeks of preparation. Dilution series of the compounds were made in PBS, pH 6.9. Diluted compound (100 μl) was added to the well of a 96-well plate; then 50 μl of 400 ng/ml recombinant human sialidase NEU3 (TP316537; Origene) in PBS, pH 6.9, was added to each well (50 μl PBS, pH 6.9, for the control); and the plate was incubated for 30 minutes at 37°C. Fifty microliters of 800 ng/ml L-TGF-β1 (299-LT/CF; R&D Systems) in PBS, pH 6.9, was then added to the well. The plate was covered with aluminum foil and incubated for 2 hours at 37°C, and released active TGF-β1 was assayed as described above.

Inhibition of NEU3 Induced Interleukin-6 Accumulation. Dilutions of the above compounds were made in serum-free medium prepared as previously described (Pilling et al., 2009b; Karhadkar et al., 2020), 50 μl of diluted compound was added to the well of a 96-well plate, then 50 μl of 400 ng/ml sialidase in serum-free medium was added to each well (50 μl serum-free medium for control), and the plate was incubated for 30 minutes at 37°C in a humidified incubator with 5% CO_2. PBMCs (100 μl) at 1×10^5 cells/ml were then added to the well to make the total volume in a well 200 μl with 1×10^4 cells/well, and this was incubated at 37°C in a humidified incubator with 5% CO_2 for 24 or 48 hours. Interleukin-6 (IL-6) in the culture supernatant was then assayed with an IL-6 ELISA kit (430501; BioLegend, San Diego, CA) following the manufacturer's protocol, reading absorbance with a SynergyMX plate reader (BioTek). At least three different donors were used for each assay.

Mouse Model of Pulmonary Fibrosis. To determine whether the NEU3 inhibitors affect pulmonary fibrosis in mice, 8–10-week-old 26–30 g male C57BL/6 mice (Jackson Laboratories, Bar Harbor, ME) were given an oropharyngeal aspiration of 3 U/kg bleomycin (2246-10; BioVision Incorporated, Milpitas, CA) in 50 μl of 0.9% saline to induce symptoms of pulmonary fibrosis or oropharyngeal saline alone as a control as previously described (Pilling and Gomer, 2014; Pilling et al., 2014; Cox et al., 2015). Starting 10 days after bleomycin had been administered, some of the bleomycin-treated mice were given daily intraperitoneal injections of 100 μl of PBS or 1 mg/kg 2-acetyl pyridine, 1 mg/kg methyl picolinate, or 0.1 mg/kg of 4-amino-1-methyl-2-piperidinecarboxylic acid in 100 μl PBS. All mice were weighed daily for 21 days after bleomycin was administered. At day 21, mice were euthanized by CO_2 inhalation, and bronchoalveolar lavage (BAL) fluid and cell spots of BAL cells were obtained as previously described (Daubeuf and Frossard, 2012; Pilling and Gomer, 2014; Pilling et al., 2014; Cox et al., 2015). The liver, heart, kidneys, spleen, white fat tissue, and brown fat tissue were removed and weighed. The total cells from BAL cell spots were quantified as described previously (Daubeuf and Frossard, 2012; Pilling and Gomer, 2014). The lungs were removed and inflated with Surgipath frozen section compound (3801480; Leica, Buffalo Grove, IL) and preserved at −80°C. Cryosections of lungs (6–10 μm) were placed on glass slides (48311-703; VWR) and were air-dried for 48 hours before use. The mouse experiments were performed in accordance with the recommendations in the Guide for the Care and Use of Laboratory Animals of National Institutes of Health. The Texas A&M University Animal Use and Care Committee approved the protocol (IACUC 2017-0414 (Institutional Animal Care And Use Committee 2017-0414)).

Histology, Immunohistochemistry, and BAL Analysis. Air-dried cryosections were stained with hematoxylin and eosin or with Sirus red to detect collagen or with 1 μg/ml antiactive TGF-β1 antibodies (AB-100-NA; R&D Systems) as described previously (Pilling et al., 2007; Karhadkar et al., 2017). The staining was quantified with ImageJ (Schneider et al., 2012; Jensen, 2013). Immunohistochemistry on BAL cell spots and cryosections was performed as described previously (Pilling and Gomer, 2014; Pilling et al., 2014; Cox et al., 2015; Karhadkar et al., 2020) using anti-CD11b (101202, clone M1/70 BioLegend) to detect blood and inflammatory macrophages, anti-CD11c (M100-3, clone 223H7; MBL International, Woburn, MA) to detect alveolar macrophages and dendritic cells, anti-CD45 (103102, clone 30-F11; BioLegend) for total leukocytes, anti-Ly-6G (127602, clone 1A8; BioLegend) to detect neutrophils,

Downloaded from jpet.aspetjournals.org at ASPET Journals on April 19, 2024

and anti-Ly-6C (128001, clone HK1.4; BioLegend) to detect a variety of inflammatory immune system cells, with isotype-matched irrelevant antibodies (BioLegend) as controls. SDS-PAGE analysis of BAL and nanodrop protein assays were performed as described previously (Pilling et al., 2003; Karhadkar et al., 2017, 2020). Western blots stained for albumin were done as described previously (Karhadkar et al., 2020).

Hydroxyproline Assay. Hydroxyproline assays were performed as described previously (Karhadkar et al., 2020) with the exception that approximately half of lobes of lungs frozen in optimal cutting temperature compound (OCT; Fisher) were cut off in three pieces, thawed, and washed three times with 0.5 ml PBS to remove optimal cutting temperature by centrifugation at 2000*g* for 5 minutes in preweighed Eppendorf tubes. After the last centrifugation, the tubes were kept inverted for 5 minutes to allow PBS to blot onto blotting paper, and the tissue was then weighed. Tissues were then processed using a hydroxyproline quantification kit (MAK008-1KT; Sigma-Aldrich) following the manufacturer's directions.

Statistics. Data were analyzed by *t* test or ANOVA using Prism 7 (GraphPad, La Jolla, CA). Significance was defined as $P < 0.05$. IC_{50} curves for enzyme assays were generated using the dose response–inhibition curve-fitting model with variable slope with Prism 7. Based on previously analyzed confidence intervals and historical data and using G*Power power analysis software (Faul et al., 2007, 2009), a sample size of three mice per group was determined sufficient to detect the effect sizes anticipated in the present experiments.

Results

Recombinant Human NEU3 Desialylates Recombinant Human LAP and Releases Active TGF-β1. Neuraminidases from influenza virus and bacteria remove sialic acid from the LAP protein, which causes the LAP to release active TGF-β1 (Schultz-Cherry and Hinshaw, 1996; Carlson et al., 2010; Gratz et al., 2017). To determine the effect of recombinant human sialidases on recombinant human LAP (rhLAP), we incubated recombinant human sialidases (made in HEK293 cells) or *C. perfringens* neuraminidase (Cox et al., 2015) with rhLAP. Western blots of the rhLAP were stained with *Sambucus nigra* lectin to detect sialic acids (Shibuya et al., 1987; Feng et al., 2013). NEU3, NEU4, and *C. perfringens* neuraminidase significantly decreased sialic acid on rhLAP (Fig. 1, A and B).

We previously found that the addition of recombinant human NEU3 (rhNEU3) to human immune cells, pulmonary fibroblasts, and small airway epithelial cells causes them to upregulate extracellular and intracellular TGF-β1 (Karhadkar et al., 2017). To determine whether NEU3 causes recombinant human latent TGF-β1 (rhL-TGF-β1) to release active TGF-β1, we incubated rhL-TGF-β1 with rhNEU3 and measured released active TGF-β1. rhNEU3 did cause a release of active TGF-β (Fig. 1C). In the presence or absence of calcium [which potentiates the activity of some viral sialidases (Dimmock, 1971; Shtyrya et al., 2009)], rhNEU1 or rhNEU2 did not cause significant release of active TGF-β1 (Supplemental Fig. 2, A and B). rhNEU3 and *C. perfringens* neuraminidase released active TGF-β1, and NEU4 caused some release of TGF-β1 (Supplemental Fig. 2, A and B). Together, these results suggest that NEU3 removes sialic acid from the LAP protein and efficiently releases active TGF-β1 from rhL-TGF-β1.

The standard assay for sialidases is cleavage of the fluorogenic substrate 4MU-NANA (Potier et al., 1979). At concentrations of rhNEU3 up to 100 ng/ml (1.94 nM) and

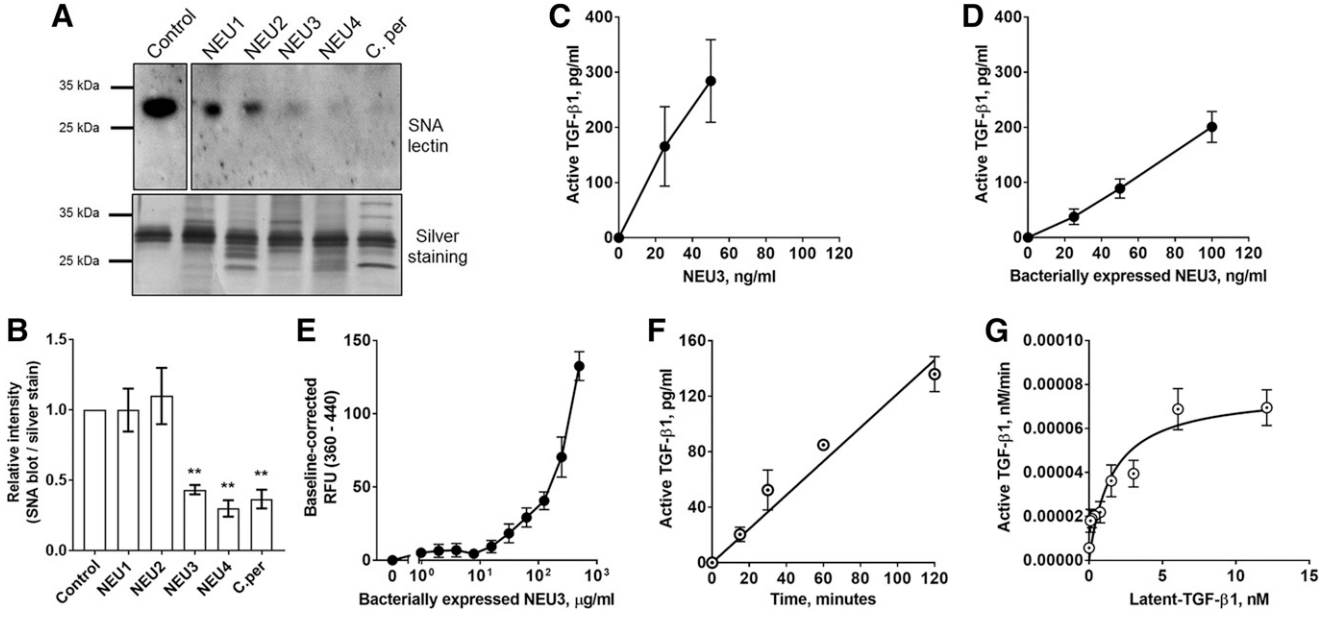

Fig. 1. Recombinant human NEU3 releases active TGF-β1 by desialylating recombinant human LAP. (A) Recombinant human LAP protein was incubated with or without recombinant human sialidases NEU1–4 or *C. perfringens* (C. per) neuraminidase, and a Western blot was stained with *S. nigra* lectin (SNA) (top panel) to detect sialic acids on glycoconjugates. Black bands are the LAP protein. Silver staining (bottom panel) was done as a loading control. Blots and silver staining are representative of three independent experiments. Degradation products from the sialidases are also visible in the silver-stained gel in addition to the LAP protein. (B) The Western blots from (A) were quantified for *S. nigra* staining of LAP protein. Values are mean ± S.E.M., $n = 3$. $^{**}P \leq 0.01$ (one-way ANOVA, Bonferroni's test compared with control). (C) An ELISA assay, specific for active TGF-β1, was performed on rhL-TGF-β1 treated with the indicated concentrations of recombinant human NEU3. Values are mean ± S.E.M., $n = 6$. Purified bacterially expressed recombinant human MBP-NEU3 was assayed for effects on (D) rhL-TGF-β1 and (E) hydrolysis of the substrate 4MU-NANA to release fluorophore 4MU (4-Methylumbelliferone). Values are mean ± S.E.M., $n \geq 3$. RFU - Relative fluorescence units. (F) Release of active TGF-β1 as a function of time by 1.94 nM recombinant human NEU3 from 3 nM rhL-TGF-β1. Values are mean ± S.E.M., $n = 4$. (G) Kinetics of recombinant human NEU3 activity in the TGF-β1 release assay. Values are mean ± S.E.M., $n = 4$.

Downloaded from jpet.aspetjournals.org at ASPET Journals on April 19, 2024

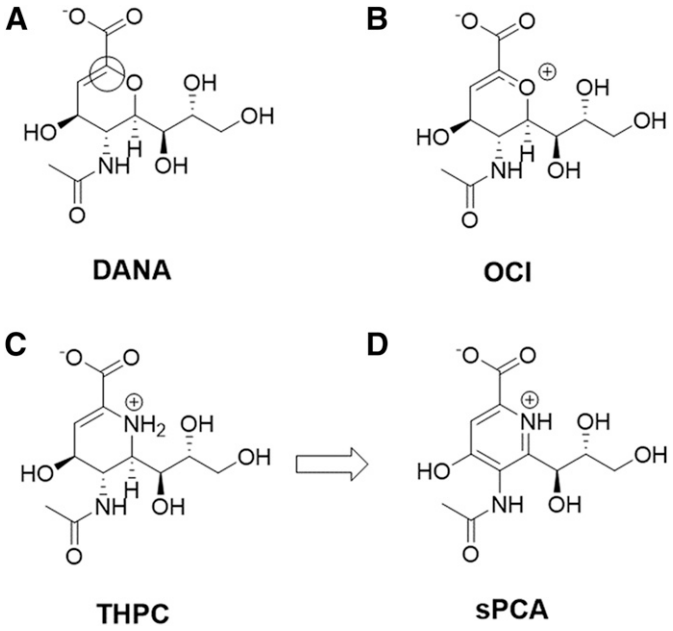

Fig. 2. Schematic representation of the rationale for design of NEU3 inhibitors. Structures of (A) DANA, (B) the predicted OCI, (C) tetrahydropyridine-1-ium-2-carboxylate (THPC), and (D) a substituted picolinic acid analog of OCI (sPCA).

using 4MU-NANA with no enzyme as a control, we were unable to detect statistically significant activity of rhNEU3 on 4MU-NANA. Compared with commercially available HEK293 cell–synthesized rhNEU3, we were able to purify much higher amounts of a bacterially expressed fusion of the 42 kDa maltose-binding protein with the 51 kDa human NEU3 (brhNEU3; bacterially expressed recombinant human NEU3); Supplemental Fig. 3, A and B). The ~93 kDa brhNEU3 contained a contaminant band that stained weakly for NEU3 on Western blots (Supplemental Fig. 3, A and B), so the concentration of bhrNEU3 was estimated by comparison of the ~93-kDa band to BSA standards on silver-stained gels. The brhNEU3 caused a release of active TGF-β1 from rhL-TGF-β1, albeit with somewhat lower efficacy than rhNEU3 (Fig. 1, C and D). Compared with rhL-TGF-β1 as a substrate, a much higher concentration of brhNEU3 was required to obtain detectable cleavage of 4MU-NANA (Fig. 1, C–E).

A previous study with 4MU-NANA as the substrate for NEU3 reported a K_m of 45 ± 3 μM and a k_{cat} of 0.33 ± 0.02 minute^{-1} and thus a catalytic efficiency k_{cat}/K_m of 0.007 ± 0.006 μM^{-1} minute^{-1} (Albohy et al., 2010). Using rhL-TGF-β1 as the substrate for rhNEU3 and measuring the rate of TGF-β1 release for different concentrations of rhL-TGF-β1 (Fig. 1, F and G), we observed a K_m of 1.5 ± 0.5 nM and a k_{cat} of (4.0 ± 0.4) × 10^{-5} minute^{-1} (both mean ± S.E.M., n = 4) and thus a k_{cat}/K_m of 0.026 ± 0.008 μM^{-1} minute^{-1}. The lower K_m and higher k_{cat}/K_m for rhL-TGF-β1 compared with 4MU-NANA suggest a higher affinity of NEU3 for rhL-TGF-β1 compared with 4MU-NANA as a substrate. Together, these results suggest that rhL-TGF-β1 can be used as a better substrate than 4MU-NANA for a more sensitive assay to determine NEU3 activity.

Design of NEU3 Inhibitors. We designed possible inhibitors of human NEU3 based in part on the structure of DANA (Fig. 2A), a known inhibitor of NEU3 (K_i = 30 μM) (Albohy et al., 2011). DANA contains a double bond, of which the sp^2-hybridized carbon-2 (circled) may be a structural mimic of the putative oxacarbenium ion intermediate (OCI) (Fig. 2, A and B) of the chemical mechanism of enzymatic catalysis (Albohy et al., 2010). Because DANA lacks the positive charge of the OCI, a better mimic of this putative reaction intermediate is likely afforded by the tetrahydropyridine-1-ium-2-carboxylate (Fig. 2C), which provides the positive charge with retention of sp^2-hybridized carbon-2. Consequently, we pursued substituted picolinic acids, which contain both a cationic nitrogen atom and sp^2-hybridization at carbon-2 (Fig. 2D) as well as a substituted pipecolinic acid (compounds 3–5 in Table 1).

Compounds 3–5 Inhibit NEU3 Release of TGF-β1. To test the hypothesis that compounds 3–5 inhibit NEU3, we assayed their effects in the rhNEU3–rhL-TGF-β1 release of active TGF-β1 reaction (Supplemental Fig. 4; Table 1). Picolinates like 2AP and MP had higher potencies of inhibiting rhNEU3 activity compared with DANA and oseltamivir phosphate (Tamiflu) (Supplemental Fig. 4, A–D and F–I; Table 1), which supported our rationale for potential NEU3 inhibitors. The fully saturated pipecolinic acid compound, AMPCA, was also a very potent inhibitor of NEU3 (Supplemental Fig. 4, E and J; Table 1) despite its lack of an adjacent sp^2-hybridized carbon as in the case of the picolinate inhibitors. These results suggest the cationic nitrogen and an adjacent keto or carboxylate group provided the essential structural elements to effect potent inhibition of rhNEU3, possibly via mimicry of the enzymatic transition state structure, and that these inhibitors are significantly improved over DANA and oseltamivir when rhL-TGF-β1 is the substrate.

Compounds 3–5 Inhibit NEU3-Induced Extracellular Accumulation of IL-6 by Human Immune Cells. rhNEU3 upregulates extracellular accumulation of IL-6 from human PBMCs (Karhadkar et al., 2020). To determine whether other sialidases have an effect on IL-6 production by PBMCs, we cultured human PBMCs with recombinant human NEU1–4 and measured extracellular accumulation of IL-6 in media supernatants after 24 and 48 hours. At 48 hours, compared with controls only rhNEU3 significantly upregulated extracellular accumulation of IL-6 (Supplemental Fig. 5). We measured the effects of inhibitors in an NEU3-induced IL-6 release by human immune cells assay (Supplemental Fig. 6; Table 1). DANA, Tamiflu, 2AP, and MP all inhibited rhNEU3 in the cell-based NEU3-induced IL-6 release assay (Supplemental Fig. 6, A–D and F–I; Table 1). Compared with the other compounds, the pipecolinate AMPCA had an increased inhibition potency (Supplemental Fig. 6, E and J; Table 1). These results

TABLE 1

Compounds used in NEU3 activity assays

List of commercially available compounds used in the NEU3-induced release of active TGF-β1 assay and the cell-based NEU3-induced upregulation of IL-6 assay to determine IC_{50}. The IC_{50} values are mean ± S.E.M., $n \geq 3$.

No.	Compound Name	Compound Structure	IC_{50}, μM	
			TGF-β1 Assay	IL-6 Assay
1	DANA		>100	7.4 ± 3.7
2	Oseltamivir phosphate (Tamiflu)		0.51 ± 0.34	0.020 ± 0.001
3	2AP		0.040 ± 0.006	19.1 ± 2.9
4	MP		<0.002	0.47 ± 0.08
5	AMPCA		<0.002	<0.002

Downloaded from jpet.aspetjournals.org at ASPET Journals on April 19, 2024

suggest that some picolinates and a pipecolinate can be used as inhibitors against NEU3 in cell-based or in vivo assays. The differences in inhibition potencies in the cell-based extracellular IL-6 accumulation assay and in vitro TGF-β1–based assay may be due to the presence or absence of factors that interact with NEU3 and/or the inhibitors in the cell-based IL-6 assay compared with the buffer-based TGF-β1 release assay.

NEU3 Inhibitors Inhibit Mouse NEU3. To determine whether compounds 3–5 would be effective in mice, we tested them against recombinant mouse NEU3 in the NEU3-induced release of active TGF-β1 assay. The IC_{50} of 2AP was 0.8 ± 1.7 μM, MP was 3.2 ± 1.6 nM, and AMPCA was less than 1 nM (Supplemental Fig. 7, A–F). These results suggest that the three selected NEU3 inhibitors are inhibitors of mouse NEU3.

AMPCA Attenuates Weight Loss of Mice after Bleomycin Treatment. To determine whether NEU3 inhibitors affect bleomycin-induced pulmonary fibrosis, C57BL/6 mice were treated with an oropharyngeal aspiration of saline or bleomycin, and then starting 10 days after saline or bleomycin, mice were given daily intraperitoneal injections of 1 mg/kg 2AP or MP or 0.1 mg/kg AMPCA. There was no discernable effect of any of the compounds on the appearance or behavior of the mice. As previously observed, compared with saline-treated control mice, bleomycin-treated control mice had lower body weights at day 21 after bleomycin aspiration (Fig. 3A). In saline-treated mice, 2AP, MP, and AMPCA did not significantly affect body weights. AMPCA attenuated the bleomycin-induced weight loss (Fig. 3A). 2AP, MP, and AMPCA did not significantly affect liver, heart, kidneys, spleen, white fat, or brown fat weights as a percent of total body weight (Supplemental Fig. 8, A–F). There was no discernable effect of any of the compounds on the appearance of any internal organs other than the lungs, which had large white patches with bleomycin alone and a normal pink color with the inhibitors without bleomycin. With bleomycin, the lungs of mice treated with 2AP or AMPCA were a normal pink color and showed occasional small white patches in mice treated with MP. Together these results suggest that AMPCA attenuates bleomycin-induced weight loss in mice.

AMPCA Attenuates Protein Increase in the BAL Fluid at Day 21 after Bleomycin Treatment. Bleomycin causes an increase in protein levels in the BAL fluid from mouse lungs (Parker and Townsley, 2004; Kulkarni et al., 2013; Pilling and Gomer, 2014). To determine whether inhibiting NEU3 affects these BAL protein levels, we measured the protein in the BAL as a measure of lung tissue damage post–bleomycin treatment. As observed previously (Parker and Townsley, 2004; Kulkarni et al., 2013; Pilling and Gomer, 2014; Karhadkar et al., 2020), at day 21, compared with saline-treated control mice, bleomycin-treated control mice showed upregulated BAL protein levels (Fig. 3, B–D). Compared with saline-treated control,

Downloaded from jpet.aspetjournals.org at ASPET Journals on April 19, 2024

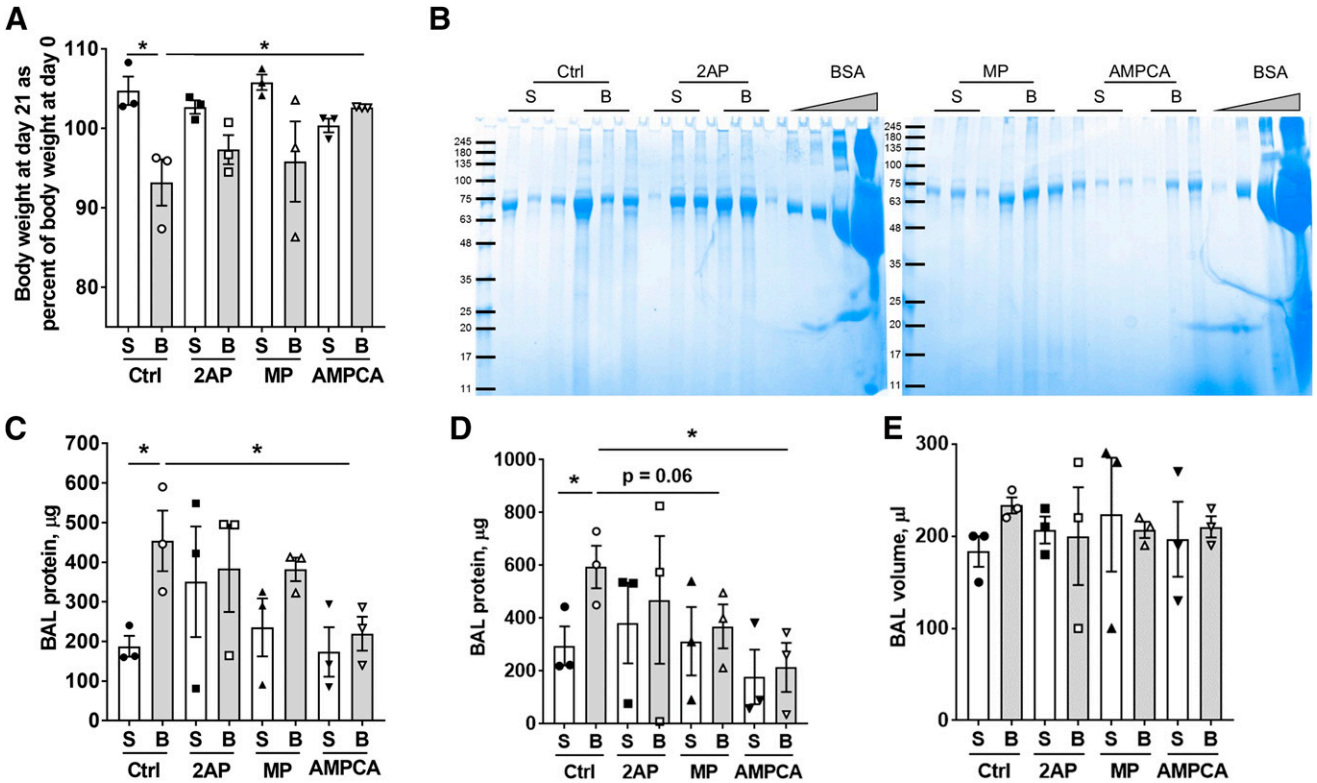

Fig. 3. AMPCA attenuates bleomycin-induced decline in body weight and protein increase in the BAL fluid at day 21 after bleomycin treatment. (A) Percent change in body weight after saline (S) or bleomycin (B) treatment at day 0 and then at day 10 starting daily intraperitoneal injections of PBS (Ctrl), 2AP, MP, or AMPCA. Values are mean ± S.E.M., $n = 3$. *$P \leq 0.05$ (t test). BAL fluid was collected at day 21 after saline or bleomycin treatment and 2AP, MP, or AMPCA intraperitoneal injections. (B) BAL fluids from the indicated mice were analyzed by PAGE gels stained with Coomassie. Molecular mass markers in kDa are at left and in the center. BSA at 0.01, 0.1, 1.0, and 10.0 μg was loaded at right on each gel. (C) Quantification of protein by densitometry in lanes from (A), using the BSA band densities as standards and then for each mouse multiplying by the BAL volume to obtain total BAL protein. (D) Quantification of protein from BAL as in (B) using a nanodrop assay to obtain BAL protein concentrations and then for each mouse multiplying by the BAL volume to obtain total BAL protein. For (B and C), values are mean ± S.E.M., $n = 3$. *$P < 0.05$ (t test). (E) BAL volumes. Values are mean ± S.E.M., $n = 3$.

the saline-treated 2AP-, MP-, or AMPCA-injected mice had no significant difference in the levels of proteins in the BAL as assayed by either gel densitometry (Fig. 3, B and C) or nanodrop (Fig. 3D). AMPCA treatment significantly attenuated the bleomycin-induced increase of protein levels in the BAL (Fig. 3, B–D). Although 2AP and MP seemed to decrease BAL protein levels in bleomycin-treated mice, the effect was not statistically significant. As reported previously (Parker and Townsley, 2004; Karhadkar et al., 2020), the bleomycin-induced protein in BAL appeared to be mainly albumin, which was confirmed by an immunoblot with anti-albumin antibodies (Supplemental Fig. 9, A and B). No significant differences were observed in the BAL volumes from the mice in the different groups (Fig. 3E). We previously observed that Tamiflu treatment but not DANA treatment attenuated bleomycin-induced increased protein levels in the BAL (Karhadkar et al., 2017). Together, these results suggest that some NEU3 inhibitors can attenuate bleomycin-induced upregulation of protein levels in the BAL.

NEU3 Inhibitors Attenuate the Increased Number of Inflammatory Cells in the BAL at Day 21 after Bleomycin Treatment. Bleomycin aspiration also causes an upregulation of inflammatory cells in the BAL at day 21 (Murray et al., 2010; Pilling and Gomer, 2014; Pilling et al., 2014; Cox et al., 2015). Compared with saline-treated control mice, the bleomycin-treated control mice showed upregulated BAL cell counts (Fig. 4A). The saline-treated control mice and and saline-treated and 2AP-, MP-, or AMPCA-injected mice showed similar BAL cell counts (Fig. 4A). Compared with saline-treated mice, bleomycin-treated and MP- or AMPCA-injected mice showed upregulated BAL cell counts, but these were significantly less compared with bleomycin-treated control mice (Fig. 4A). In the BAL of bleomycin-treated control mice, as previously observed (Karhadkar et al., 2020), bleomycin increased the number of CD11b+ cells (Fig. 4 B), CD11c+ cells (Fig. 4C), CD45+ cells (Fig. 4D), and Ly6G positive cells (Fig. 4E). Significant differences were not observed for Ly6C positive cells (Fig. 4F). The BAL of saline-treated control mice and saline-treated and 2AP-, MP-, or AMPCA-treated mice showed similar counts of the above cell types (Fig. 4, B–F). Compared with BAL from saline-treated mice, bleomycin-treated 2AP- or AMPCA-injected mice showed upregulated counts of CD11b positive cells (Fig. 4B), CD11c positive cells (Fig. 4C), and CD45 positive cells (Fig. 4D) in the BAL, but these counts were significantly less compared with bleomycin-treated control mice. The MP-injected mice did not show significantly increased counts of the above cell types in the BAL of saline-treated or bleomycin-treated mice (Fig. 4, B–F). Together, these data suggest that NEU3 inhibitors attenuate the bleomycin-induced increase of inflammatory cell counts in the BAL.

Lung sections were also stained to detect inflammatory cells. As previously observed (Karhadkar et al., 2020), bleomycin increased the counts of CD11b+, CD11c+, and CD45+ cells remaining in the lungs after BAL (Fig. 5, A–C) but did not affect the counts of Ly6G+ or Ly6C+ cells (Fig. 5, D–E). 2AP, MP, or AMPCA did not affect the counts of CD11b+ and CD11c+ cells (Fig. 5, A and B), but 2AP and MP significantly counteracted the increase in CD45+ cells in the lungs after BAL at day 21 (Fig. 5C). Together, these results suggest that some NEU3 inhibitors attenuate the upregulation of some

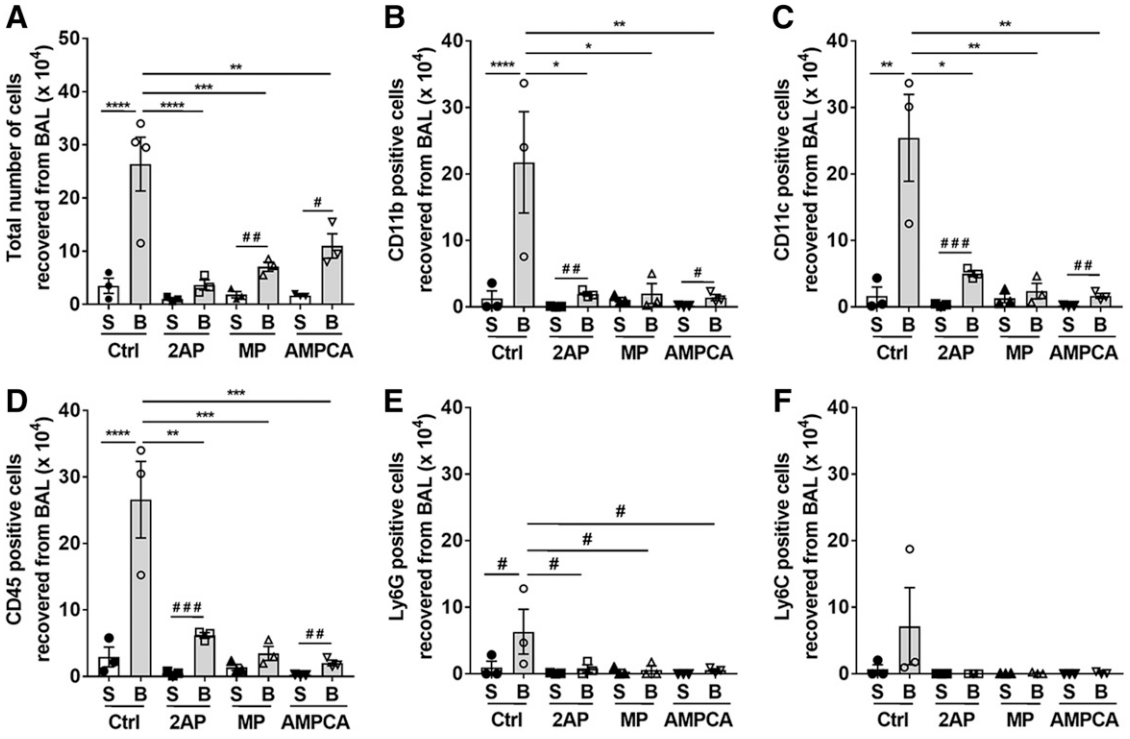

Fig. 4. 2AP, MP, or AMPCA from day 10 after bleomycin treatment decrease BAL cells. (A) The total number of cells in mouse BAL after the indicated treatment. S indicates saline and B indicates bleomycin. Values are mean ± S.E.M., $n \geq 3$ mice per group. $^{**}P < 0.01$; $^{***}P < 0.001$; $^{****}P < 0.0001$ (one-way ANOVA, Bonferroni's test). $\#P < 0.05$; $\#\#P < 0.01$ (t test). BAL cell spots at day 21 were stained for the markers (B) CD11b, (C) CD11c, (D) CD45, (E) Ly6G, and (F) Ly6C. The percent of cells stained was determined in five randomly chosen fields of 100–150 cells, and the percentage was multiplied by the total number of BAL cells for that mouse to obtain the total number of BAL cells staining for the marker. Values are mean ± S.E.M., $n = 3$. $^{*}P < 0.05$; $^{***}P < 0.001$; $^{****}P < 0.0001$ (one-way ANOVA, Bonferroni's test). $\#P < 0.05$; $\#\#P < 0.01$; $\#\#\#P < 0.001$ (t test). Ctrl, Control.

Downloaded from jpet.aspetjournals.org at ASPET Journals on April 19, 2024

leukocytes remaining in the lungs after BAL at day 21 post–bleomycin treatment.

NEU3 Inhibitors Decrease Fibrosis. To determine whether inhibiting NEU3 can decrease bleomycin-induced fibrosis, lung sections were stained with hematoxylin and eosin to detect tissue and picrosirius red to detect total collagen, and hydroxyproline levels were measured in the lung tissue lysates. As previously observed (Adamson and Bowden, 1974; Izbicki et al., 2002; Walters and Kleeberger, 2008; Moore et al., 2013), bleomycin treatment caused fibrosis in the mouse lungs at day 21 (Fig. 6, A–D and Supplemental Fig. 10). Compared with saline treatment, lungs from mice exposed to bleomycin and then treated with MP showed increased Sirius red staining and hydroxyproline levels at day 21 (Fig. 6, B–D). The Sirius red staining and hydroxyproline levels from bleomycin-treated and then 2AP-, MP-, or AMPCA-treated mice were significantly less than those from the bleomycin-treated control mice (Fig. 6, C and D; Supplemental Fig. 10). The bleomycin-treated and then 2AP-, MP-, or AMPCA-treated mice showed reduced staining for active TGF-β1 in the lung sections compared with bleomycin-treated control mice (Fig. 7, A and B). These results suggest that NEU3 inhibitors reduce bleomycin-induced fibrosis and TGF-β1 upregulation in mouse lungs.

Discussion

In this report, we observed that the human sialidase NEU3 desialylates human LAP and causes release of active TGF-β1. This is in agreement with the observation that LAP desialylation by viral and bacterial sialidases (Carlson et al., 2010; Gratz et al., 2017) causes a conformational modification of the LAP, which results in disruption of the interaction between LAP and active TGF-β1, releasing active TGF-β1 (Biernacka et al., 2011). Compared with the more conventional mechanism of a cell sensing a signal and activating a gene expression pathway to make and secrete a responding signal, the desialylation of LAP and release of active TGF-β1 are a much more rapid response. This then suggests that fibrosis is associated with a mechanism that originally evolved to rapidly respond to an insult, such as a sialidase-expressing pathogen, with the extracellular NEU3 mimicking and thus amplifying the pathogen signal.

NEU1 may also be involved in potentiating pulmonary fibrosis (Luzina et al., 2016), but this sialidase did not significantly desialylate LAP, cause TGF-β1 release, or induce IL-6 accumulation by PBMCs, suggesting that it may act by other mechanisms to promote fibrosis. NEU2 also did not significantly desialylate LAP, cause TGF-β1 release, or induce IL-6 accumulation by PBMCs. NEU4 did desialylate LAP and caused modest amounts of TGF-β1 release and IL-6 accumulation, but since this sialidase is present in lysosomes (Seyrantepe et al., 2004) or mitochondria and endoplasmic reticulum (Yamaguchi et al., 2005; Bigi et al., 2010), it either does not normally desialylate LAP or NEU4 from necrotic or otherwise lysed cells may normally desialylate LAP.

We used a predicted reaction intermediate from the NEU3 reaction mechanism (Albohy et al., 2010, 2011) to test the idea that picolinic acid–like compounds containing a cationic nitrogen replacing the putative positively charged oxygen of the reaction intermediate could act as NEU3 inhibitors. In both the TGF-β1 release from LAP and the IL-6 production by PBMC assays, we observed significantly improved inhibition potency of AMPCA compared with DANA or oseltamivir (Table 1). Since some tumors have upregulated NEU3 (Kakugawa et al., 2002; Nomura et al., 2006; Ueno et al., 2006;

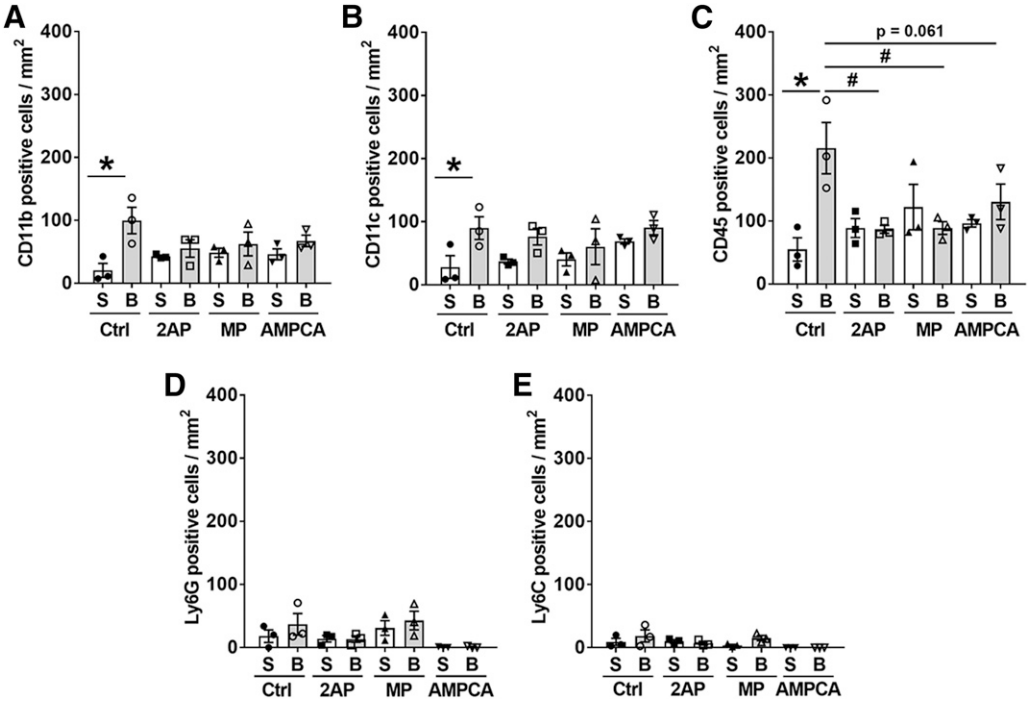

Fig. 5. Remaining immune cells in lungs post-BAL. Cryosections of mouse lungs were stained for (A) CD11b, (B) CD11c, (C) CD45, (D) Ly6G, and (E) Ly6C, and cells in five randomly chosen 0.45 mm–diameter fields of view were counted, and the number was then calculated to number per squared millimeter. Values are mean ± S.E.M., $n = 3$. *$P < 0.05$ (one-way ANOVA, Bonferroni's test). #$P < 0.05$ (t test). B, bleomycin; S, saline

Downloaded from jpet.aspetjournals.org at ASPET Journals on April 19, 2024

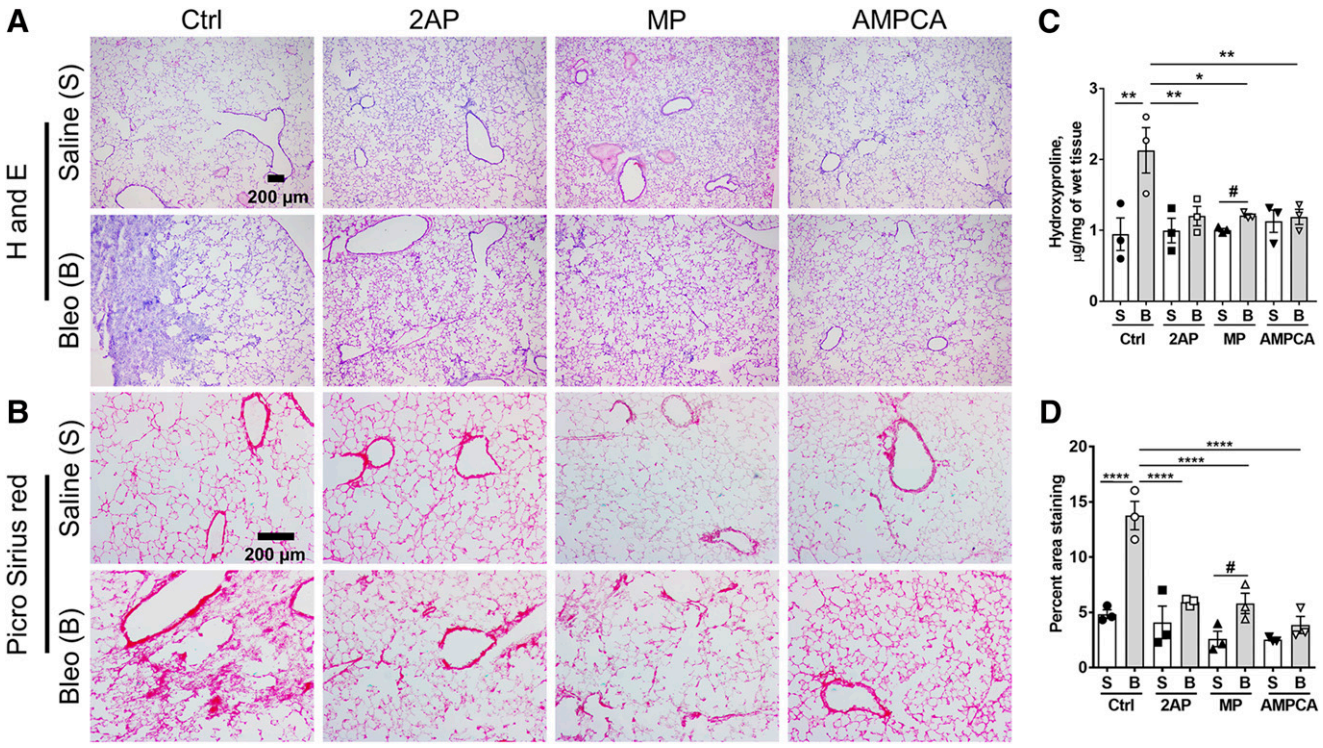

Fig. 6. 2AP, MP, or AMPCA injections starting at day 10 after bleomycin (Bleo) attenuate fibrosis. Sections of lung tissue from mice treated with saline or bleomycin, then injected daily with control or 2AP or MP or AMPCA starting at day 10 after bleomycin, and then euthanized at day 21 were stained with (A) H&E and (B) picrosirius red to show collagen content. All images are representative of three mice per group. (C) Hydroxyproline in lungs. Values are mean ± S.E.M., $n = 3$. *$P < 0.05$; **$P < 0.01$ (one-way ANOVA, Bonferroni's test). #$P < 0.05$ (t test). (D) Picrosirius red quantification analyzed by selecting five random fields of view of the sizes shown in (B) for each mouse, and the avg. percent area of the field of view showing staining for each mouse was measured. Values are mean ± S.E.M., $n = 3$. ****$P < 0.0001$ (one-way ANOVA, Bonferroni's test). #$P < 0.05$ (t test). Ctrl, Control.

Kawamura et al., 2012) and since mice lacking Neu3 are resistant to colitis-associated colon tumor formation (Yamaguchi et al., 2012), AMPCA or similar picolinate compounds may useful to treat NEU3-associated tumors.

In support of the idea of using picolinate compounds against NEU3-associated tumors, a previous study found antiproliferative and therapeutic effects of picolinic acid on tumor cells (Ruffmann et al., 1987). Picolinic acid shows cytotoxic activity against virus-infected cells and also decreases viral replication (Fernandez-Pol and Johnson, 1977; Fernandez-Pol et al., 2001). Picolinic acid potentiates the antimicrobial activities of various fluoroquinolones by chelating metal ions (Cai et al., 2006; Shimizu and Tomioka, 2006). Picolinic acid functions as a second signal in enhancing interferon-γ–induced macrophage activation (Varesio et al., 1990; Melillo et al., 1994) and has neuroprotective, immune regulatory, and tumor suppression effects in human

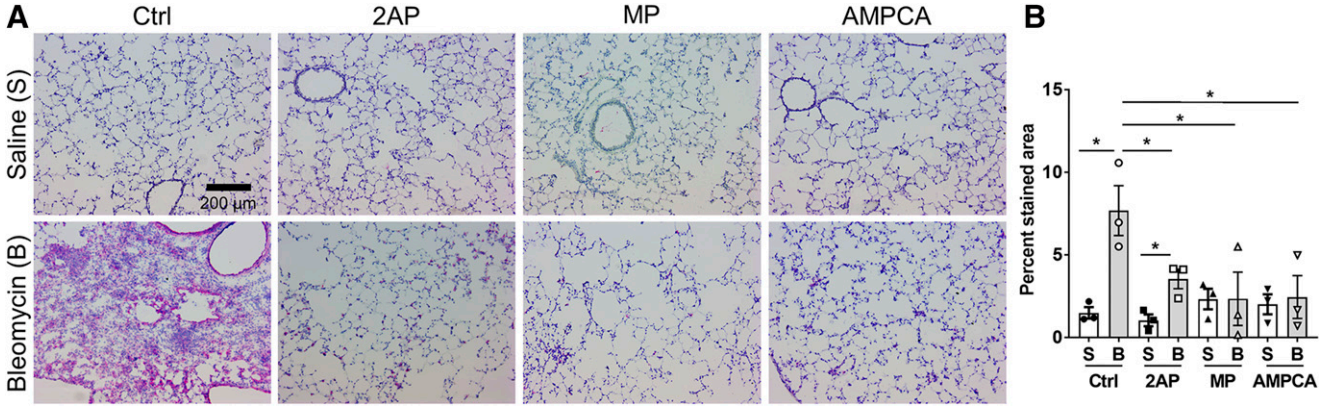

Fig. 7. 2AP, MP, or AMPCA injections starting at day 10 after bleomycin reduces TGF-β1 staining. (A) Sections of lung tissue from mice treated with saline or bleomycin, then injected daily with control or 2AP or MP or AMPCA starting at day 10 after bleomycin, and then euthanized at day 21 were stained with antibodies against TGF-β1. All images are representative of three mice per group. Pink is staining, blue is counterstain. (B) Quantification of staining analyzed by selecting three random fields of view of the sizes shown in (A) for each mouse, and the avg. percent area of the field of view showing staining for each mouse was measured. Values are mean ± S.E.M., $n = 3$. *$P < 0.05$ (t test). B, bleomycin; S, saline; Ctrl, Control.

Downloaded from jpet.aspetjournals.org at ASPET Journals on April 19, 2024

neurons (Guillemin et al., 2007). These reports, and our studies suggest that picolinic acid, a metabolite of tryptophan degradation (Varesio et al., 1990; Badawy, 2017), and picolinates may be useful as therapeutics.

NEU1 and NEU2 did not significantly desialylate LAP or release active TGF-β1 from rhL-TGF-β1, and thus this assay was incompatible for determining inhibition potencies of our compounds against NEU1 and NEU2. The extracellular pH of lesions in lung fibrosis ranges from 6.45 to 6.95 (Jones et al., 2015). Our repeated efforts to assay NEU1, NEU2, and NEU4 in this pH range with the substrate 4MU-NANA were unsuccessful. Thus, it is unclear whether our compounds inhibit sialidases other than NEU3. One test of the specificity of the inhibitors would be to test them for their ability to inhibit fibrosis in mice lacking NEU3, but since mice lacking NEU3 do not develop fibrosis in the bleomycin model (Karhadkar et al., 2020), this cannot be done, and we thus cannot rule out the possibility that the inhibitors inhibit fibrosis through some mechanism not involving NEU3.

As with AMPCA, DANA and Tamiflu attenuated bleomycin-induced protein upregulation in the BAL at day 21 (Karhadkar et al., 2017). However, 2AP or MP did not significantly attenuate bleomycin-induced protein upregulation in BAL at day 21. These disparate results may be due to dose effects or effects that DANA, Tamiflu, 2AP, MP, and AMPCA have on targets other than NEU3.

We previously observed that NEU3 is upregulated in the mouse bleomycin model and that inhibition of sialidases with DANA or oseltamivir or loss of NEU3 attenuates bleomycin-induced pulmonary fibrosis in mice (Karhadkar et al., 2017, 2020). The human and mouse NEU3 inhibitors 2AP, MP, and AMPCA all inhibited pulmonary inflammation, levels of active TGF-β1 in the lungs, and pulmonary fibrosis in the mouse bleomycin model. The UniProt sequences P01137 for human L-TGF-β1 and P04202 for mouse L-TGF-β1 show 90% amino acid sequence similarity and conserved glycosylation sites (Pruitt et al., 2007; Areström et al., 2012; Doğan et al., 2016; UniProt Consortium, 2019). A reasonable explanation for the ability of NEU3 inhibitors to decrease bleomycin-induced increased levels of active TGF-β1 is that mouse NEU3 also desialylates mouse LAP to release mouse TGF-β1. Together, these results support the hypothesis that a positive feedback loop in which NEU3 desialylates LAP to release active TGF-β1 and the active TGF-β1 causes lung epithelial cells to increase translation of *NEU3* mRNA and decrease degradation of NEU3 protein (Chen et al., 2020) contributes to pulmonary fibrosis and suggest that NEU3 inhibitors are potential therapeutics for pulmonary fibrosis.

Acknowledgments

We thank Darrell Pilling for assistance with BAL sample collection and the LARR (Laboratory Animal Resources and Research) staff at Texas A&M for animal care. We also thank Kristen Consalvo, Wensheng Chen, and Darrell Pilling for comments on the manuscript.

Authorship Contributions

Participated in research design: Karhadkar, Meek, Gomer.

Conducted experiments: Karhadkar.

Performed data analysis: Karhadkar, Meek, Gomer.

Wrote or contributed to the writing of the manuscript: Karhadkar, Meek, Gomer.

References

Adamson IY and Bowden DH (1974) The pathogenesis of bleomycin-induced pulmonary fibrosis in mice. *Am J Pathol* **77**:185–197.

Albohy A, Li MD, Zheng RB, Zou C, and Cairo CW (2010) Insight into substrate recognition and catalysis by the human neuraminidase 3 (NEU3) through molecular modeling and site-directed mutagenesis. *Glycobiology* **20**:1127–1138.

Albohy A, Mohan S, Zheng RB, Pinto BM, and Cairo CW (2011) Inhibitor selectivity of a new class of oseltamivir analogs against viral neuraminidase over human neuraminidase enzymes. *Bioorg Med Chem* **19**:2817–2822.

Anthony RM and Ravetch JV (2010) A novel role for the IgG Fc glycan: the anti-inflammatory activity of sialylated IgG Fcs. *J Clin Immunol* **30** (Suppl 1):S9–S14.

Areström I, Zuber B, Bengtsson T, and Ahlborg N (2012) Measurement of human latent Transforming Growth Factor-β1 using a latency associated protein-reactive ELISA. *J Immunol Methods* **379**:23–29.

Badawy AA (2017) Kynurenine pathway of tryptophan metabolism: regulatory and functional aspects. *Int J Tryptophan Res* **10**:1178646917691938.

Biernacka A, Dobaczewski M, and Frangogiannis NG (2011) TGF-β signaling in fibrosis. *Growth Factors* **29**:196–202.

Bigi A, Morosi L, Pozzi C, Forcella M, Tettamanti G, Venerando B, Monti E, and Fusi P (2010) Human sialidase NEU4 long and short are extrinsic proteins bound to outer mitochondrial membrane and the endoplasmic reticulum, respectively. *Glycobiology* **20**:148–157.

Blackwell TS, Tager AM, Borok Z, Moore BB, Schwartz DA, Anstrom KJ, Bar-Joseph Z, Bitterman P, Blackburn MR, Bradford W, et al. (2014) Future directions in idiopathic pulmonary fibrosis research. An NHLBI workshop report. *Am J Respir Crit Care Med* **189**:214–222.

Cai S, Sato K, Shimizu T, Yamabe S, Hiraki M, Sano C, and Tomioka H (2006) Antimicrobial activity of picolinic acid against extracellular and intracellular Mycobacterium avium complex and its combined activity with clarithromycin, rifampicin and fluoroquinolones. *J Antimicrob Chemother* **57**:85–93.

Cairo CW (2014) Inhibitors of the human neuraminidase enzymes. *MedChemComm* **5**:1067–1074.

Carlson CM, Turpin EA, Moser LA, O'Brien KB, Cline TD, Jones JC, Tumpey TM, Katz JM, Kelley LA, Gauldie J, et al. (2010) Transforming growth factor-β: activation by neuraminidase and role in highly pathogenic H5N1 influenza pathogenesis. *PLoS Pathog* **6**:e1001136.

Chen W, Lamb TM, and Gomer RH (2020) TGF-β1 increases sialidase 3 expression in human lung epithelial cells by decreasing its degradation and upregulating its translation. *Exp Lung Res* **46**:75–80.

Cox N, Pilling D, and Gomer RH (2015) DC-SIGN activation mediates the differential effects of SAP and CRP on the innate immune system and inhibits fibrosis in mice. *Proc Natl Acad Sci USA* **112**:8385–8390.

Crawford SE, Stellmach V, Murphy-Ullrich JE, Ribeiro SM, Lawler J, Hynes RO, Boivin GP, and Bouck N (1998) Thrombospondin-1 is a major activator of TGF-beta1 in vivo. *Cell* **93**:1159–1170.

Cutroneo KR, White SL, Phan SH, and Ehrlich HP (2007) Therapies for bleomycin induced lung fibrosis through regulation of TGF-beta1 induced collagen gene expression. *J Cell Physiol* **211**:585–589.

Daubeuf F and Frossard N (2012) Performing bronchoalveolar lavage in the mouse. *Curr Protoc Mouse Biol* **2**:167–175.

Dimmock NJ (1971) Dependence of the activity of an influenza virus neuraminidase upon Ca2+. *J Gen Virol* **13**:481–483.

Doğan T, MacDougall A, Saidi R, Poggioli D, Bateman A, O'Donovan C, and Martin MJ (2016) UniProt-DAAC: domain architecture alignment and classification, a new method for automatic functional annotation in UniProtKB. *Bioinformatics* **32**:2264–2271.

Faul F, Erdfelder E, Buchner A, and Lang A-G (2009) Statistical power analyses using G*Power 3.1: tests for correlation and regression analyses. *Behav Res Methods* **41**:1149–1160.

Faul F, Erdfelder E, Lang A-G, and Buchner A (2007) G*Power 3: a flexible statistical power analysis program for the social, behavioral, and biomedical sciences. *Behav Res Methods* **39**:175–191.

Feng C, Zhang L, Nguyen C, Vogel SN, Goldblum SE, Blackwelder WC, and Cross AS (2013) Neuraminidase reprograms lung tissue and potentiates lipopolysaccharide-induced acute lung injury in mice. *J Immunol* **191**:4828–4837.

Fernandez IE and Eickelberg O (2012) The impact of TGF-β on lung fibrosis: from targeting to biomarkers. *Proc Am Thorac Soc* **9**:111–116.

Fernandez-Pol JA and Johnson GS (1977) Selective toxicity induced by picolinic acid in simian virus 40-transformed cells in tissue culture. *Cancer Res* **37**:4276–4279.

Fernandez-Pol JA, Klos DJ, and Hamilton PD (2001) Antiviral, cytotoxic and apoptotic activities of picolinic acid on human immunodeficiency virus-1 and human herpes simplex virus-2 infected cells. *Anticancer Res* **21**:3773–3776.

Gratz N, Loh LN, Mann B, Gao G, Carter R, Rosch J, and Tuomanen EI (2017) Pneumococcal neuraminidase activates TGF-β signalling. *Microbiology (Reading)* **163**:1198–1207.

Guillemin GJ, Cullen KM, Lim CK, Smythe GA, Garner B, Kapoor V, Takikawa O, and Brew BJ (2007) Characterization of the kynurenine pathway in human neurons. *J Neurosci* **27**:12884–12892.

Guo T, Dätwyler P, Demina E, Richards MR, Ge P, Zou C, Zheng R, Fougerat A, Pshezhetsky AV, Ernst B, et al. (2018) Selective inhibitors of human neuraminidase 3. *J Med Chem* **61**:1990–2008.

Hata K, Koseki K, Yamaguchi K, Moriya S, Suzuki Y, Yingsakmongkon S, Hirai G, Sodeoka M, von Itzstein M, and Miyagi T (2008) Limited inhibitory effects of oseltamivir and zanamivir on human sialidases. *Antimicrob Agents Chemother* **52**:3484–3491.

Hayden FG, Osterhaus ADME, Treanor JJ, Fleming DM, Aoki FY, Nicholson KG, Bohnen AM, Hirst HM, Keene O, and Wightman K (1997) Efficacy and safety of the neuraminidase inhibitor zanamivir in the treatment of influenzavirus infections. GG167 Influenza Study Group. *N Engl J Med* **337**:874–880.

Downloaded from jpet.aspetjournals.org at ASPET Journals on April 19, 2024

Hinck AP, Mueller TD, and Springer TA (2016) Structural biology and evolution of the TGF-β family. *Cold Spring Harb Perspect Biol* **8**:a022103.
Izbicki G, Or R, Christensen TG, Segel MJ, Fine A, Goldstein RH, and Breuer R (2002) Bleomycin-induced lung fibrosis in IL-4-overexpressing and knockout mice. *Am J Physiol Lung Cell Mol Physiol* **283**:L1110–L1116.
Jenkins G (2008) The role of proteases in transforming growth factor-beta activation. *Int J Biochem Cell Biol* **40**:1068–1078.
Jensen EC (2013) Quantitative analysis of histological staining and fluorescence using ImageJ. *Anat Rec (Hoboken)* **296**:378–381.
Jobling MF, Mott JD, Finnegan MT, Jurukovski V, Erickson AC, Walian PJ, Taylor SE, Ledbetter S, Lawrence CM, Rifkin DB, et al. (2006) Isoform-specific activation of latent transforming growth factor beta (LTGF-beta) by reactive oxygen species. *Radiat Res* **166**:839–848.
Jones KM, Randtke EA, Howison CM, Cárdenas-Rodríguez J, Sime PJ, Kottmann RM, and Pagel MD (2015) Measuring extracellular pH in a lung fibrosis model with acidoCEST MRI. *Mol Imaging Biol* **17**:177–184.
Kakugawa Y, Wada T, Yamaguchi K, Yamanami H, Ouchi K, Sato I, and Miyagi T (2002) Up-regulation of plasma membrane-associated ganglioside sialidase (Neu3) in human colon cancer and its involvement in apoptosis suppression. *Proc Natl Acad Sci USA* **99**:10718–10723.
Karhadkar TR, Chen W, and Gomer RH (2020) Attenuated pulmonary fibrosis in sialidase-3 knockout (*Neu3*$^{-/-}$) mice. *Am J Physiol Lung Cell Mol Physiol* **318**: L165–L179.
Karhadkar TR, Pilling D, Cox N, and Gomer RH (2017) Sialidase inhibitors attenuate pulmonary fibrosis in a mouse model. *Sci Rep* **7**:15069.
Kawamura S, Sato I, Wada T, Yamaguchi K, Li Y, Li D, Zhao X, Ueno S, Aoki H, Tochigi T, et al. (2012) Plasma membrane-associated sialidase (NEU3) regulates progression of prostate cancer to androgen-independent growth through modulation of androgen receptor signaling. *Cell Death Differ* **19**:170–179.
Kopitz J, Oehler C, and Cantz M (2001) Desialylation of extracellular GD1a-neoganglioprotein suggests cell surface orientation of the plasma membrane-bound ganglioside sialidase activity in human neuroblastoma cells. *FEBS Lett* **491**: 233–236.
Kulkarni AA, Thatcher TH, Hsiao H-M, Olsen KC, Kottmann RM, Morrissette J, Wright TW, Phipps RP, and Sime PJ (2013) The triterpenoid CDDO-Me inhibits bleomycin-induced lung inflammation and fibrosis. *PLoS One* **8**:e63798.
Lambré CR, Pilatte Y, Le Maho S, Greffard A, De Crémoux H, and Bignon J (1988) Sialidase activity and antibodies to sialidase-treated autologous erythrocytes in bronchoalveolar lavages from patients with idiopathic pulmonary fibrosis or sarcoidosis. *Clin Exp Immunol* **73**:230–235.
Lewandrowski U, Moebius J, Walter U, and Sickmann A (2006) Elucidation of N-glycosylation sites on human platelet proteins: a glycoproteomic approach. *Mol Cell Proteomics* **5**:226–233.
Luzina IG, Lockatell V, Hyun SW, Kopach P, Kang PH, Noor Z, Liu A, Lillehoj EP, Lee C, Miranda-Ribera A, et al. (2016) Elevated expression of NEU1 sialidase in idiopathic pulmonary fibrosis provokes pulmonary collagen deposition, lymphocytosis, and fibrosis. *Am J Physiol Lung Cell Mol Physiol* **310**:L940–L954.
Lyons RM, Keski-Oja J, and Moses HL (1988) Proteolytic activation of latent transforming growth factor-beta from fibroblast-conditioned medium. *J Cell Biol* **106**:1659–1665.
Magesh S, Suzuki T, Miyagi T, Ishida H, and Kiso M (2006) Homology modeling of human sialidase enzymes NEU1, NEU3 and NEU4 based on the crystal structure of NEU2: hints for the design of selective NEU3 inhibitors. *J Mol Graph Model* **25**: 196–207.
Mäkelä MJ, Pauksens K, Rostila T, Fleming DM, Man CY, Keene ON, and Webster A (2000) Clinical efficacy and safety of the orally inhaled neuraminidase inhibitor zanamivir in the treatment of influenza: a randomized, double-blind, placebo-controlled European study. *J Infect* **40**:42–48.
Marathe BM, Lévêque V, Klumpp K, Webster RG, and Govorkova EA (2013) Determination of neuraminidase kinetic constants using whole influenza virus preparations and correction for spectroscopic interference by a fluorogenic substrate. *PLoS One* **8**:e71401.
Martinez FJ, Collard HR, Pardo A, Raghu G, Richeldi L, Selman M, Swigris JJ, Taniguchi H, and Wells AU (2017) Idiopathic pulmonary fibrosis. *Nat Rev Dis Primers* **3**:17074.
Melillo G, Cox GW, Biragyn A, Sheffler LA, and Varesio L (1994) Regulation of nitric-oxide synthase mRNA expression by interferon-gamma and picolinic acid. *J Biol Chem* **269**:8128–8133.
Miyagi T, Takahashi K, Hata K, Shiozaki K, and Yamaguchi K (2012) Sialidase significance for cancer progression. *Glycoconj J* **29**:567–577.
Miyagi T and Yamaguchi K (2012) Mammalian sialidases: physiological and pathological roles in cellular functions. *Glycobiology* **22**:880–896.
Miyazono K and Heldin CH (1989) Role for carbohydrate structures in TGF-beta 1 latency. *Nature* **338**:158–160.
Miyazono K, Olofsson A, Colosetti P, and Heldin CH (1991) A role of the latent TGF-beta 1-binding protein in the assembly and secretion of TGF-beta 1. *EMBO J* **10**: 1091–1101.
Monto AS, Fleming DM, Henry D, de Groot R, Makela M, Klein T, Elliott M, Keene ON, and Man CY (1999) Efficacy and safety of the neuraminidase inhibitor zanamivirin the treatment of influenza A and B virus infections. *J Infect Dis* **180**:254–261.
Moore BB, Lawson WE, Oury TD, Sisson TH, Raghavendran K, and Hogaboam CM (2013) Animal models of fibrotic lung disease. *Am J Respir Cell Mol Biol* **49**: 167–179.
Moremen KW, Tiemeyer M, and Nairn AV (2012) Vertebrate protein glycosylation: diversity, synthesis and function. *Nat Rev Mol Cell Biol* **13**:448–462.
Morrissey JH (1981) Silver stain for proteins in polyacrylamide gels: a modified procedure with enhanced uniform sensitivity. *Anal Biochem* **117**:307–310.
Moscona A (2005) Neuraminidase inhibitors for influenza. *N Engl J Med* **353**: 1363–1373.
Mozzi A, Forcella M, Riva A, Difrancesco C, Molinari F, Martin V, Papini N, Bernasconi B, Nonnis S, Tedeschi G, et al. (2015) NEU3 activity enhances EGFR activation without affecting EGFR expression and acts on its sialylation levels. *Glycobiology* **25**:855–868.
Munger JS, Huang X, Kawakatsu H, Griffiths MJ, Dalton SL, Wu J, Pittet JF, Kaminski N, Garat C, Matthay MA, et al. (1999) The integrin alpha v beta 6 binds and activates latent TGF beta 1: a mechanism for regulating pulmonary inflammation and fibrosis. *Cell* **96**:319–328.
Murray LA, Rosada R, Moreira AP, Joshi A, Kramer MS, Hesson DP, Argentieri RL, Mathai S, Gulati M, Herzog EL, et al. (2010) Serum amyloid P therapeutically attenuates murine bleomycin-induced pulmonary fibrosis via its effects on macrophages. *PLoS One* **5**:e9683.
Nomura H, Tamada Y, Miyagi T, Suzuki A, Taira M, Suzuki N, Susumu N, Irimura T, and Aoki D (2006) Expression of NEU3 (plasma membrane-associated sialidase) in clear cell adenocarcinoma of the ovary: its relationship with T factor of pTNM classification. *Oncol Res* **16**:289–297.
Parker JC and Townsley MI (2004) Evaluation of lung injury in rats and mice. *Am J Physiol Lung Cell Mol Physiol* **286**:L231–L246.
Pilling D, Buckley CD, Salmon M, and Gomer RH (2003) Inhibition of fibrocyte differentiation by serum amyloid P. *J Immunol* **171**:5537–5546.
Pilling D, Fan T, Huang D, Kaul B, and Gomer RH (2009a) Identification of markers that distinguish monocyte-derived fibrocytes from monocytes, macrophages, and fibroblasts. *PLoS One* **4**:e7475.
Pilling D and Gomer RH (2014) Persistent lung inflammation and fibrosis in serum amyloid P component (APCs-/-) knockout mice. *PLoS One* **9**:e93730.
Pilling D, Roife D, Wang M, Ronkainen SD, Crawford JR, Travis EL, and Gomer RH (2007) Reduction of bleomycin-induced pulmonary fibrosis by serum amyloid P. *J Immunol* **179**:4035–4044.
Pilling D, Vakil V, and Gomer RH (2009b) Improved serum-free culture conditions for the differentiation of human and murine fibrocytes. *J Immunol Methods* **351**: 62–70.
Pilling D, Zheng Z, Vakil V, and Gomer RH (2014) Fibroblasts secrete Slit2 to inhibit fibrocyte differentiation and fibrosis. *Proc Natl Acad Sci USA* **111**:18291–18296.
Pociask DA, Sime PJ, and Brody AR (2004) Asbestos-derived reactive oxygen species activate TGF-beta1. *Lab Invest* **84**:1013–1023.
Potier M, Mameli L, Bélisle M, Dallaire L, and Melançon SB (1979) Fluorometric assay of neuraminidase with a sodium (4-methylumbelliferyl-alpha-D-N-acetylneuraminate) substrate. *Anal Biochem* **94**:287–296.
Pruitt KD, Tatusova T, and Maglott DR (2007) NCBI reference sequences (RefSeq): a curated non-redundant sequence database of genomes, transcripts and proteins. *Nucleic Acids Res* **35**:D61–D65.
Pshezhetsky AV and Ashmarina LI (2013) Desialylation of surface receptors as a new dimension in cell signaling. *Biochemistry (Mosc)* **78**:736–745.
Raghu G, Collard HR, Egan JJ, Martinez FJ, Behr J, Brown KK, Colby TV, Cordier JF, Flaherty KR, Lasky JA, et al.; ATS/ERS/JRS/ALAT Committee on Idiopathic Pulmonary Fibrosis (2011) An official ATS/ERS/JRS/ALAT statement: idiopathic pulmonary fibrosis: evidence-based guidelines for diagnosis and management. *Am J Respir Crit Care Med* **183**:788–824.
Raghu G and Selman M (2015) Nintedanib and pirfenidone. New antifibrotic treatments indicated for idiopathic pulmonary fibrosis offer hopes and raises questions. *Am J Respir Crit Care Med* **191**:252–254.
Robertson IB and Rifkin DB (2016) Regulation of the bioavailability of TGF-β and TGF-β-related proteins. *Cold Spring Harb Perspect Biol* **8**:a021907.
Rodriguez-Walker M and Daniotti JL (2017) Human sialidase Neu3 is S-acylated and behaves like an integral membrane protein. *Sci Rep* **7**:4167.
Ruffmann R, Schlick R, Chirigos MA, Budzynsky W, and Varesio L (1987) Antiproliferative activity of picolinic acid due to macrophage activation. *Drugs Exp Clin Res* **13**:607–614.
Schneider CA, Rasband WS, and Eliceiri KW (2012) NIH Image to ImageJ: 25 years of image analysis. *Nat Methods* **9**:671–675.
Schultz-Cherry S and Hinshaw VS (1996) Influenza virus neuraminidase activates latent transforming growth factor beta. *J Virol* **70**:8624–8629.
Schwab I and Nimmerjahn F (2013) Intravenous immunoglobulin therapy: how does IgG modulate the immune system? *Nat Rev Immunol* **13**:176–189.
Seyrantepe V, Landry K, Trudel S, Hassan JA, Morales CR, and Pshezhetsky AV (2004) Neu4, a novel human lysosomal lumen sialidase, confers normal phenotype to sialidosis and galactosialidosis cells. *J Biol Chem* **279**:37021–37029.
Shibuya N, Goldstein IJ, Broekaert WF, Nsimba-Lubaki M, Peeters B, and Peumans WJ (1987) The elderberry (Sambucus nigra L.) bark lectin recognizes the Neu5-Ac(alpha 2-6)Gal/GalNAc sequence. *J Biol Chem* **262**:1596–1601.
Shimizu T and Tomioka H (2006) Activity of picolinic acid in combination with the antiprotozoal drug quinacrine against Mycobacterium avium complex. *Antimicrob Agents Chemother* **50**:3186–3188.
Shtyrya YA, Mochalova LV, and Bovin NV (2009) Influenza virus neuraminidase: structure and function. *Acta Naturae* **1**:26–32.
Smutova V, Albohy A, Pan X, Korchagina E, Miyagi T, Bovin N, Cairo CW, and Pshezhetsky AV (2014) Structural basis for substrate specificity of mammalian neuraminidases. *PLoS One* **9**:e106320.
Travis MA and Sheppard D (2014) TGF-β activation and function in immunity. *Annu Rev Immunol* **32**:51–82.
Ueno S, Saito S, Wada T, Yamaguchi K, Satoh M, Arai Y, and Miyagi T (2006) Plasma membrane-associated sialidase is up-regulated in renal cell carcinoma and promotes interleukin-6-induced apoptosis suppression and cell motility. *J Biol Chem* **281**:7756–7764.
UniProt Consortium (2019) UniProt: a worldwide hub of protein knowledge. *Nucleic Acids Res* **47**:D506–D515.
van de Vlekkert D, Demmers J, Nguyen X-X, Campos Y, Machado E, Annunziata I, Hu H, Gomero E, Qiu X, Bongiovanni A, et al. (2019) Excessive exosome release is the pathogenic pathway linking a lysosomal deficiency to generalized fibrosis. *Sci Adv* **5**:eaav3270.
Varesio L, Clayton M, Blasi E, Ruffman R, and Radzioch D (1990) Picolinic acid, a catabolite of tryptophan, as the second signal in the activation of IFN-gamma-primed macrophages. *J Immunol* **145**:4265–4271.

Downloaded from jpet.aspetjournals.org at ASPET Journals on April 19, 2024

Varki A, Cummings RD, Aebi M, Packer NH, Seeberger PH, Esko JD, Stanley P, Hart G, Darvill A, Kinoshita T, et al. (2015) Symbol nomenclature for graphical representations of glycans. *Glycobiology* **25**:1323–1324.
Varki A and Gagneux P (2012) Multifarious roles of sialic acids in immunity. *Ann N Y Acad Sci* **1253**:16–36.
Varki NM and Varki A (2007) Diversity in cell surface sialic acid presentations: implications for biology and disease. *Lab Invest* **87**:851–857.
von Itzstein M (2007) The war against influenza: discovery and development of sialidase inhibitors. *Nat Rev Drug Discov* **6**:967–974.
Walters DM and Kleeberger SR (2008) Mouse models of bleomycin-induced pulmonary fibrosis. *Curr Protoc Pharmacol* **Chapter 5**:Unit 5.46.
Wolters PJ, Collard HR, and Jones KD (2014) Pathogenesis of idiopathic pulmonary fibrosis. *Annu Rev Pathol* **9**:157–179.
Wynn TA and Ramalingam TR (2012) Mechanisms of fibrosis: therapeutic translation for fibrotic disease. *Nat Med* **18**:1028–1040.
Yamaguchi K, Hata K, Koseki K, Shiozaki K, Akita H, Wada T, Moriya S, and Miyagi T (2005) Evidence for mitochondrial localization of a novel human sialidase (NEU4). *Biochem J* **390**:85–93.
Yamaguchi K, Shiozaki K, Moriya S, Koseki K, Wada T, Tateno H, Sato I, Asano M, Iwakura Y, and Miyagi T (2012) Reduced susceptibility to colitis-associated colon carcinogenesis in mice lacking plasma membrane-associated sialidase. *PLoS One* **7**:e41132.
Yue X, Shan B, and Lasky JA (2010) TGF-β: titan of lung fibrogenesis. *Curr Enzym Inhib* **6**:10.2174/10067.
Zanchetti G, Colombi P, Manzoni M, Anastasia L, Caimi L, Borsani G, Venerando B, Tettamanti G, Preti A, Monti E, et al. (2007) Sialidase NEU3 is a peripheral membrane protein localized on the cell surface and in endosomal structures. *Biochem J* **408**:211–219.
Zhou X, Yang G, and Guan F (2020) Biological functions and analytical strategies of sialic acids in tumor. *Cells* **9**:273.
Zou Y, Albohy A, Sandbhor M, and Cairo CW (2010) Inhibition of human neuraminidase 3 (NEU3) by C9-triazole derivatives of 2,3-didehydro-N-acetyl-neuraminic acid. *Bioorg Med Chem Lett* **20**:7529–7533.

Address correspondence to: Richard H. Gomer, Department of Biology, Texas A&M University, 301 Old Main Dr., College Station, TX 77843-3474. E-mail: rgomer@tamu.edu

Downloaded from jpet.aspetjournals.org at ASPET Journals on April 19, 2024

JPET-AR-2020-000258R1

Supplementary figures

Inhibiting sialidase-induced TGF-β1 activation attenuates pulmonary fibrosis in mice

Tejas R. Karhadkar [1], Thomas D. Meek [2], and Richard H. Gomer [1]

[1] Department of Biology,

[2] Department of Biochemistry and Biophysics,

Texas A&M University

301 Old Main Drive, College Station, Texas, 77843-3474 USA

Corresponding author:

Richard H Gomer

Department of Biology

Texas A&M University

301 Old Main Drive

College Station, TX 77843-3474 USA

Phone: 979-458-5745. Fax: 979-845-2891. email: rgomer@tamu.edu

Supplementary figures and supplementary figure legends

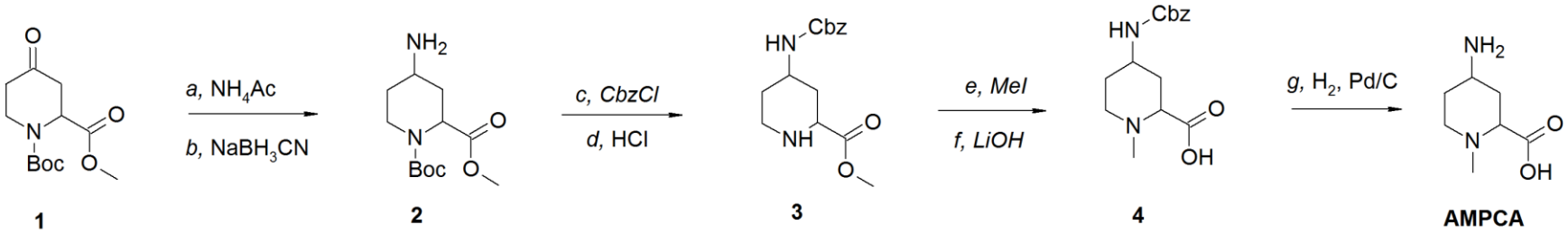

Supplementary Figure 1. Synthetic scheme for 4-amino-1-methylpiperidine-2-carboxylic acid (AMPCA). Ammonium acetate was reacted with the 4-keto group of 1-(*tert*-butyl) 2-methyl 4-oxopiperidine-1,2-dicarboxylate (**1**) to form an imine (*a*), followed by reduction (*b*) with sodium cyanoborohydride to afford the amine **2**. The installed amine was then protected by reaction with benzyloxycarbonyl chloride (*c*). The *t*-Boc group was removed by treatment with HCl (*d*), The piperidine nitrogen was then methylated in base by methyl iodide (*e*), and the methyl ester was then hydrolyzed by treatment with LiOH (*f*). The Cbz protecting group was then removed by hydrogenation catalyzed by palladium on carbon (*g*) to afford AMPCA.

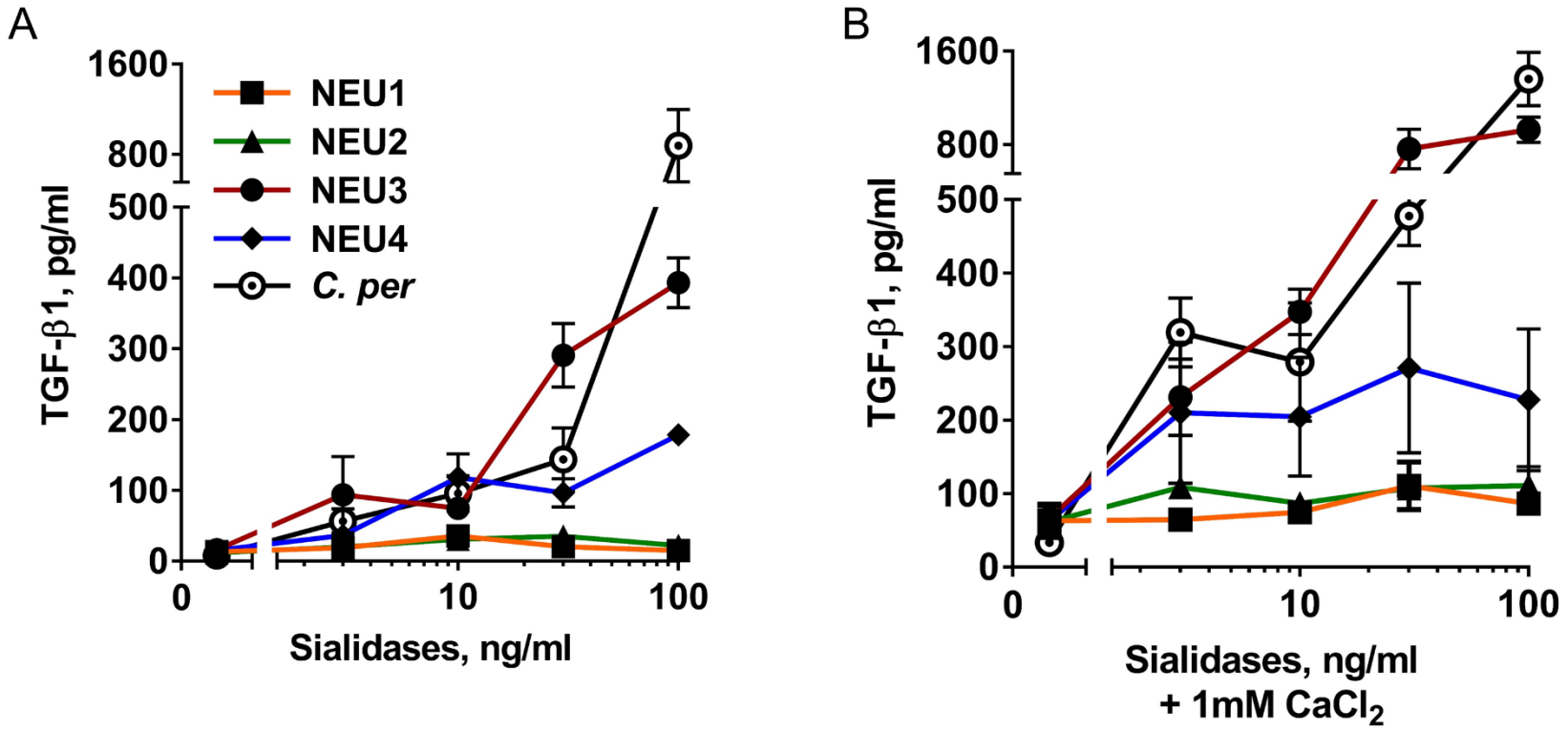

Supplementary Figure 2. Ability of sialidases to release active TGF-β1. An ELISA assay, specific for active TGF-β1, was performed on recombinant human latent-TGF-β1 (rhL-TGF-β1) treated with the indicated concentrations of NEU 1 – 4 or *C. perfringens* (*C. per*) neuraminidase in **(A)** the absence or **(B)** the presence of 1 mM $CaCl_2$. Values are mean ± SEM, n = 3.

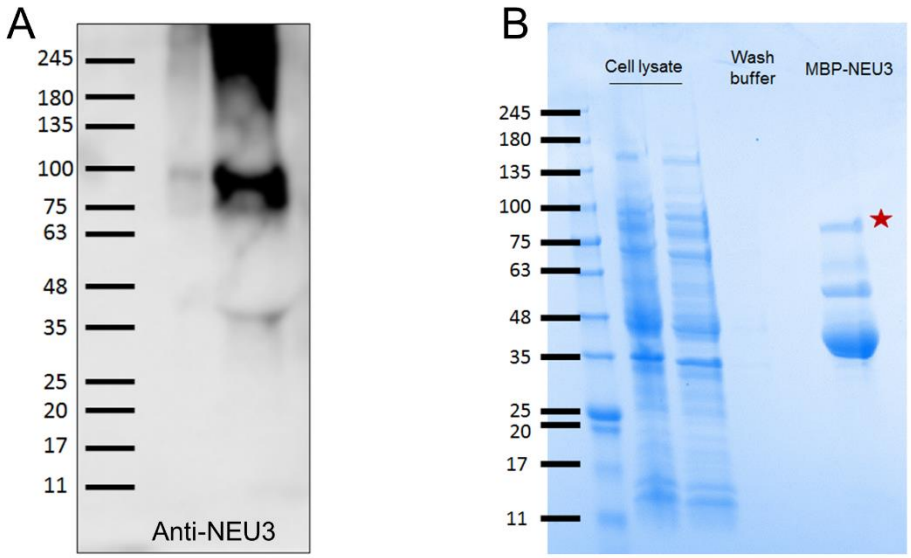

Supplementary Figure 3. Recombinant human NEU3 purified from bacteria. (A) A western blot of purified MBP-NEU3 was stained with anti-NEU3 antibodies, showing a band at the expected molecular mass of ~93 kDa, (**B)** A gel of the indicated fractions was stained with Coomassie. The desired MBP-NEU3 is marked with a star (★).

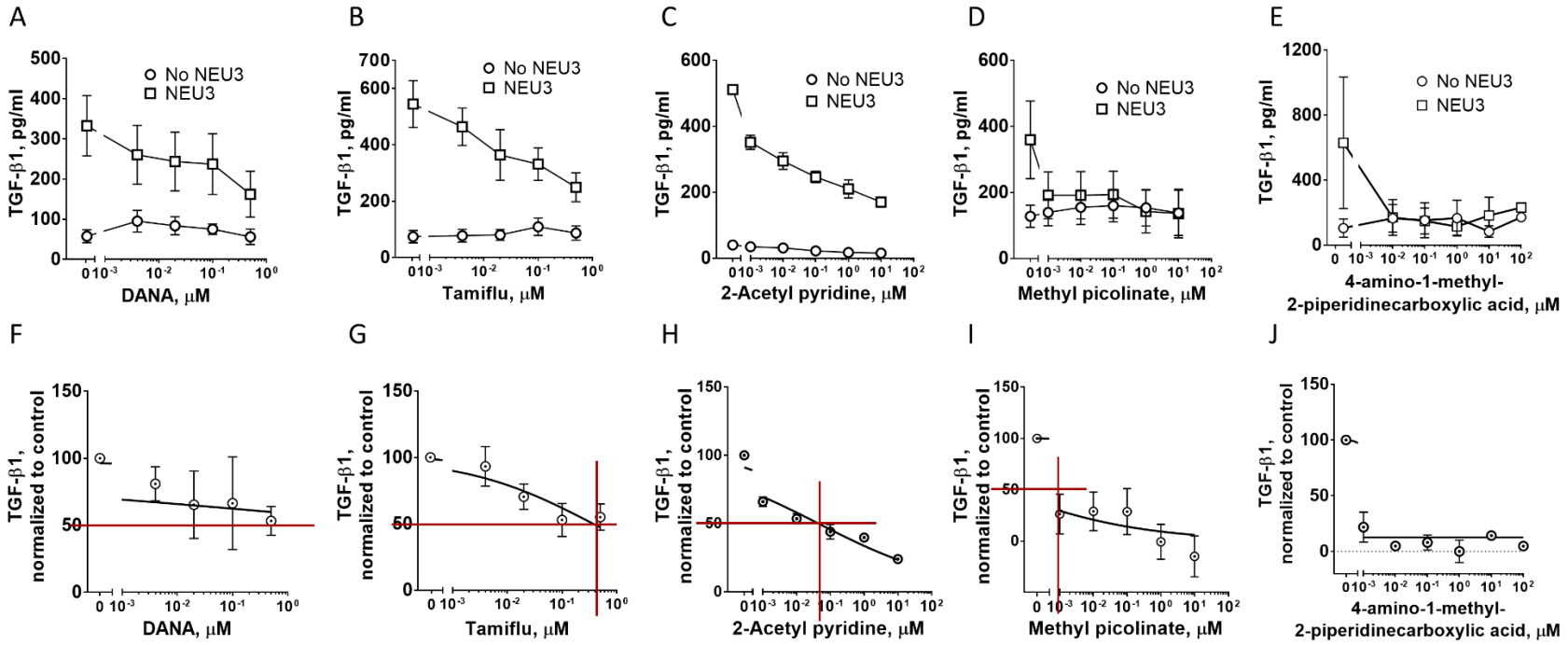

Supplementary Figure 4. Inhibition of recombinant human NEU3-catalyzed release of active TGF-β1 by compounds from Table 1. Compounds labelled on the X-axis of graphs **(A)** to **(E)** were incubated at the indicated concentrations with and without recombinant human NEU3 in PBS pH 6.9. rhL-TGF-β1 was added as substrate, and the release of active TGF-β1 was quantified by an ELISA kit. Values are mean ± SEM, n ≥ 3. The NEU3-catalyzed release of active TGF-β1 was determined by subtracting active TGF-β1 values in the absence of NEU3 from active TGF-β1 values in the presence of NEU3 in the data from (A to E). The baseline corrected values were normalized to the percent of active TGF-β1 in the absence of the compound (0 μM of inhibitor). **(F)** – **(G)** IC_{50} values (red lines) were determined from the normalized values by non-linear regression curve fitting. Values are mean ± SEM, n ≥ 3.

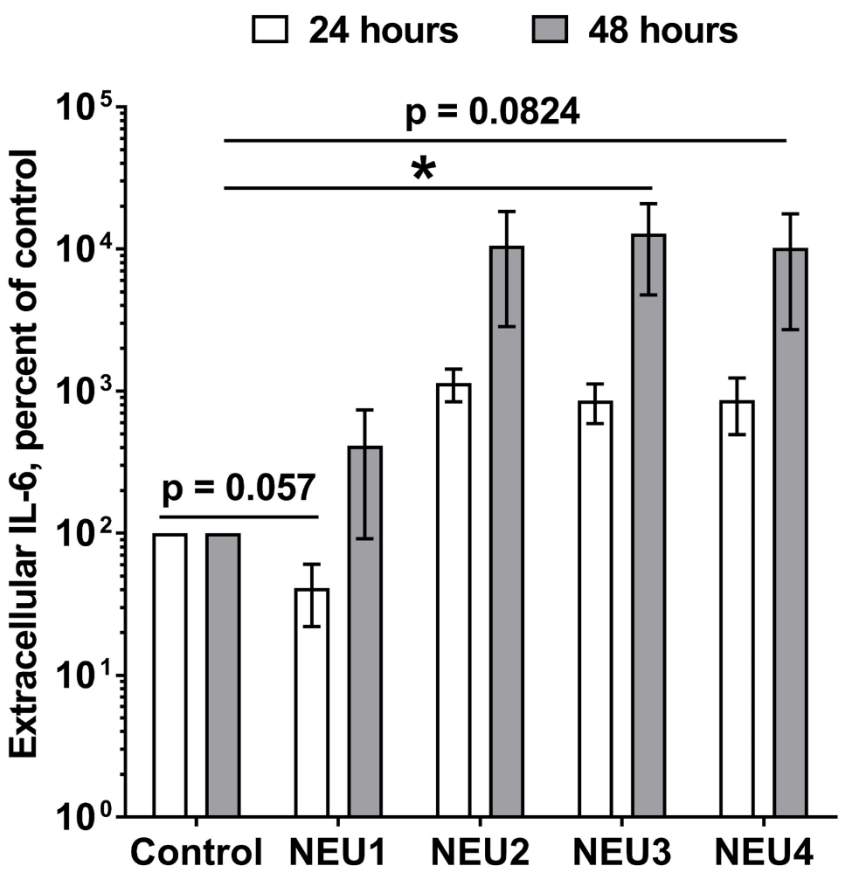

Supplementary Figure 5. The effect of sialidases on extracellular accumulation of IL-6. Human peripheral blood mononuclear cells (PBMCs) were cultured with the indicated recombinant human sialidases for 24 hours and 48 hours, and culture supernatants were assayed by ELISA for IL-6. Values are mean ± SEM, n = 3. * $p < 0.05$ (t-test).

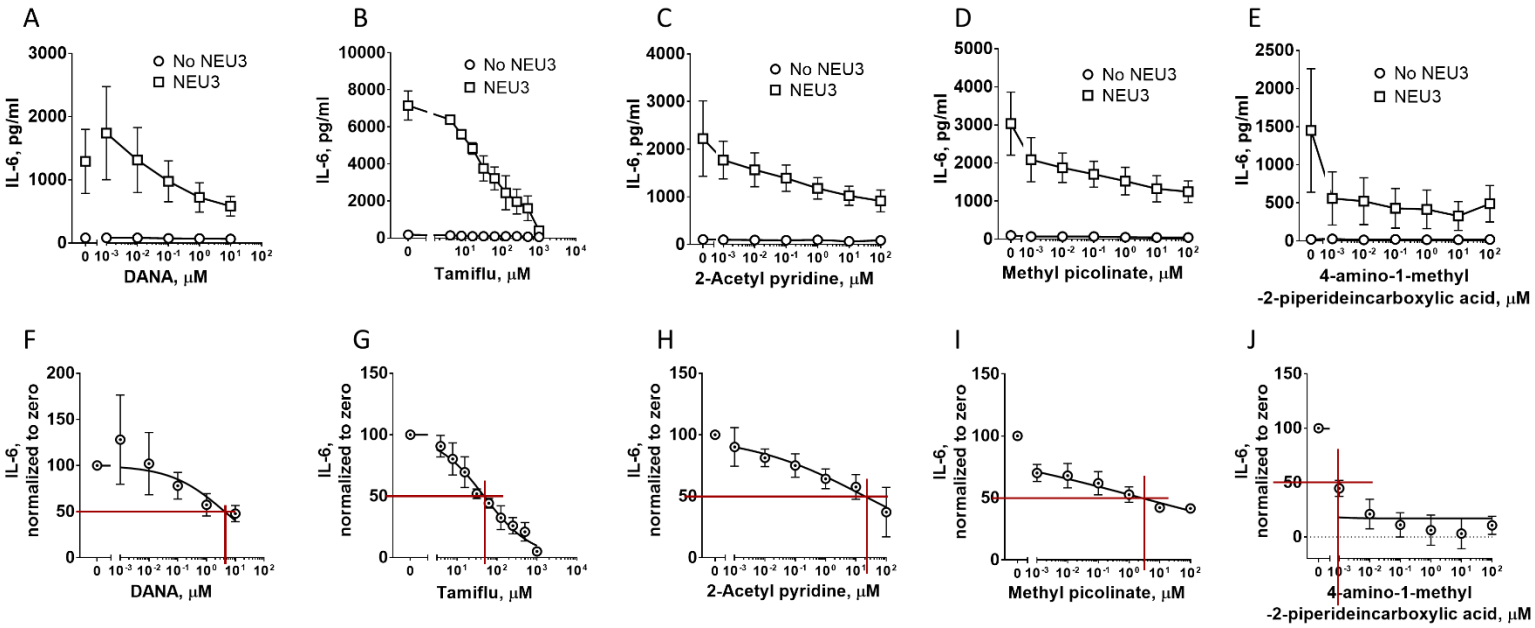

Supplementary Figure 6. Inhibition by compounds from Table 1 of recombinant human NEU3-induced extracellular accumulation of IL-6 from human PBMCs. Compounds labelled on the X-axis of graphs **(A)** to **(E)** were incubated at the indicated concentrations with and without recombinant human NEU3 in serum free media. After 30 minutes, human PBMCs were added and incubated at 37 °C, 5% CO_2. 48 hours later media supernatants were assayed for IL-6. Values are mean ± SEM, n ≥ 3. The NEU3-induced extracellular accumulation of IL-6 was determined by subtracting IL-6 values in the absence of NEU3 from IL-6 values in the presence of NEU3 in the data from (A – E). The baseline corrected values were normalized to the percent of IL-6 value in the absence of the compound (0 μM of inhibitor). **(F) – (J)**. IC_{50} values (red lines) were determined from the normalized values by non-linear regression curve fitting. Values are mean ± SEM, n ≥ 3.

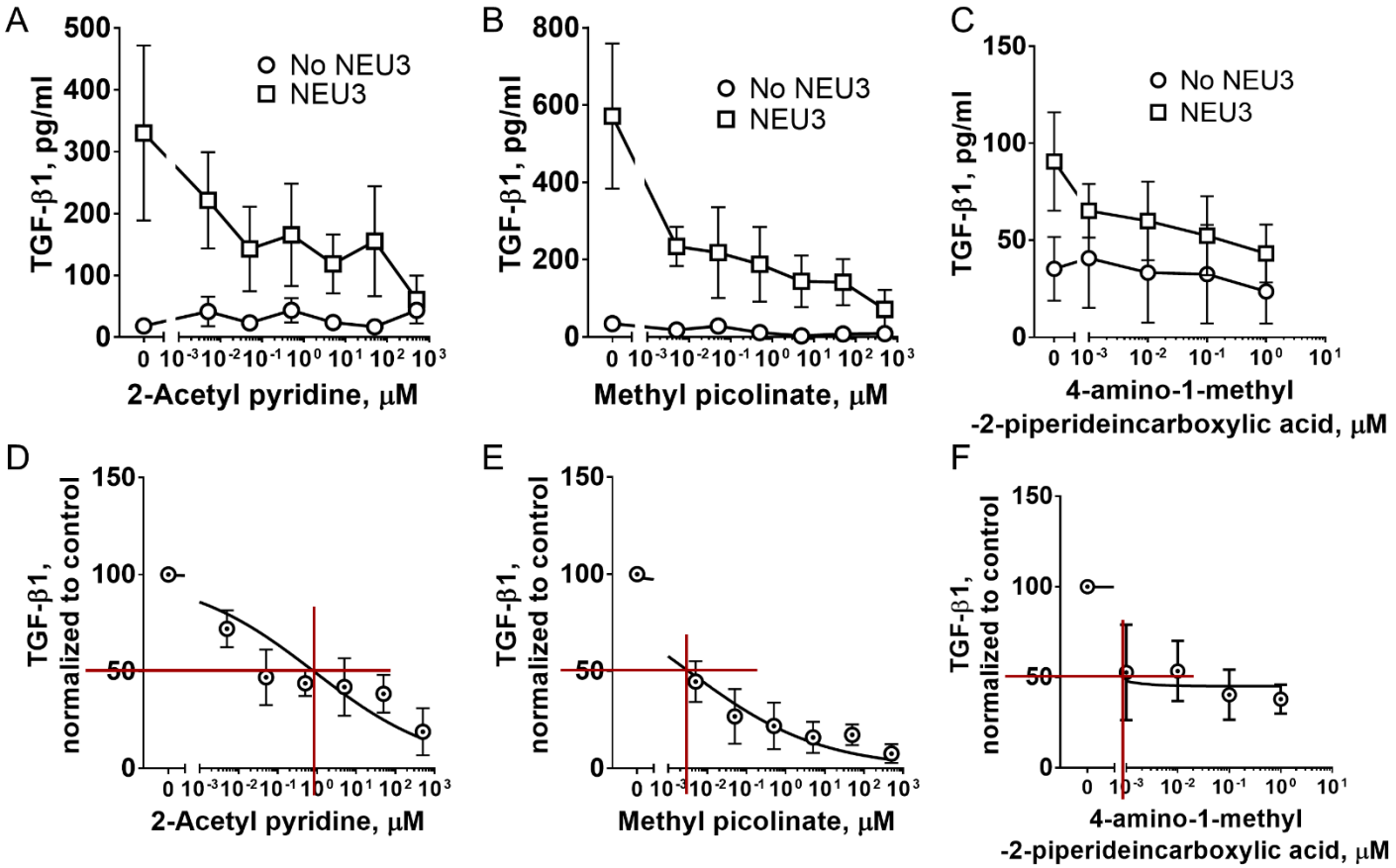

Supplementary Figure 7. NEU3 inhibitors inhibit recombinant mouse NEU3-catalyzed release of active TGF-β1. (A-C) The indicated compounds were incubated with and without recombinant mouse NEU3. rhL-TGF-β1 was added as a substrate, and the release of active TGF-β1 was quantified. Values are mean ± SEM, n ≥ 3. **(D-F)** IC_{50} values were determined as described for Supplementary Fig. 4. Values are mean ± SEM, n ≥ 3.

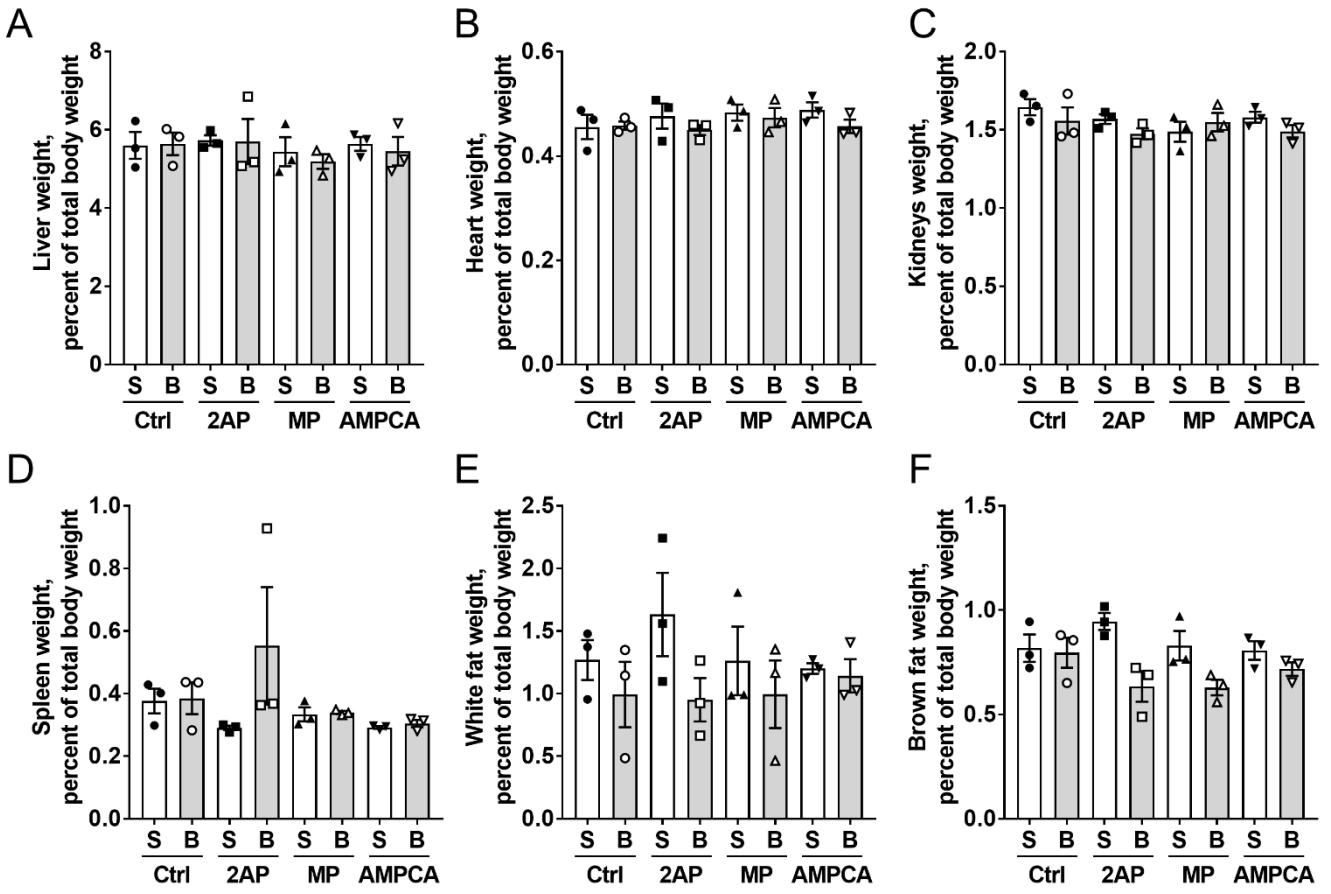

Supplementary Figure 8. Injections of 2AP, MP, or AMPCA from day 10 after bleomycin treatment had no significant effect on organ weights. Weights of **(A)** Liver, **(B)** Heart, **(C)** Kidneys, **(D)** Spleen, **(E)** White fat, and **(F)** Brown fat as percent of total body weight at day 21 after saline (S) or bleomycin (B) treatment. Values are mean ± SEM, n = 3. There were no significant changes (1way ANOVA, Bonferroni's test).

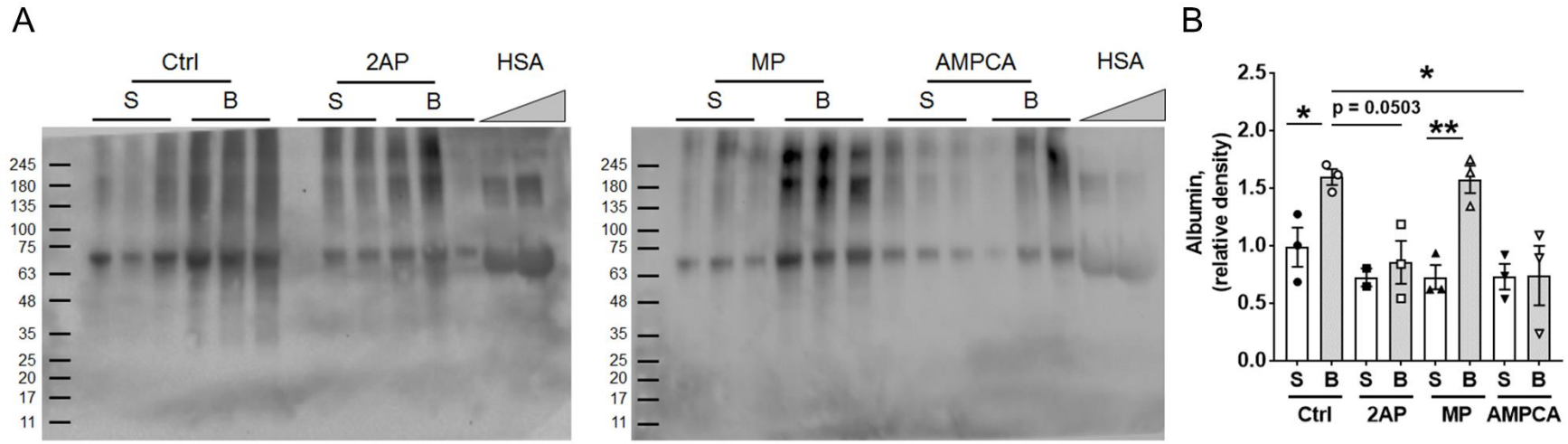

Supplementary Figure 9. AMPCA attenuates bleomycin-induced upregulation of albumin in the BAL fluid at day 21 after bleomycin treatment. (A) BAL fluids from the indicated mice were analyzed by western blots stained with anti-albumin antibodies. Molecular mass markers in kDa are at left and in the center. Human serum albumin (HSA) at 1 and 10 μg was loaded at right on each gel. **(B)** Quantification of protein by densitometry in lanes from panel A, using the BSA band densities as standards, and then for each mouse multiplying by the BAL volume to obtain relative albumin levels. S indicates saline and B indicates bleomycin. Values are mean ± SEM, n=3 except for saline aspirated and 2-acetyl pyridine (2AP) treated mice where n=2. * $p < 0.05$ and ** $p < 0.01$ (t-test).

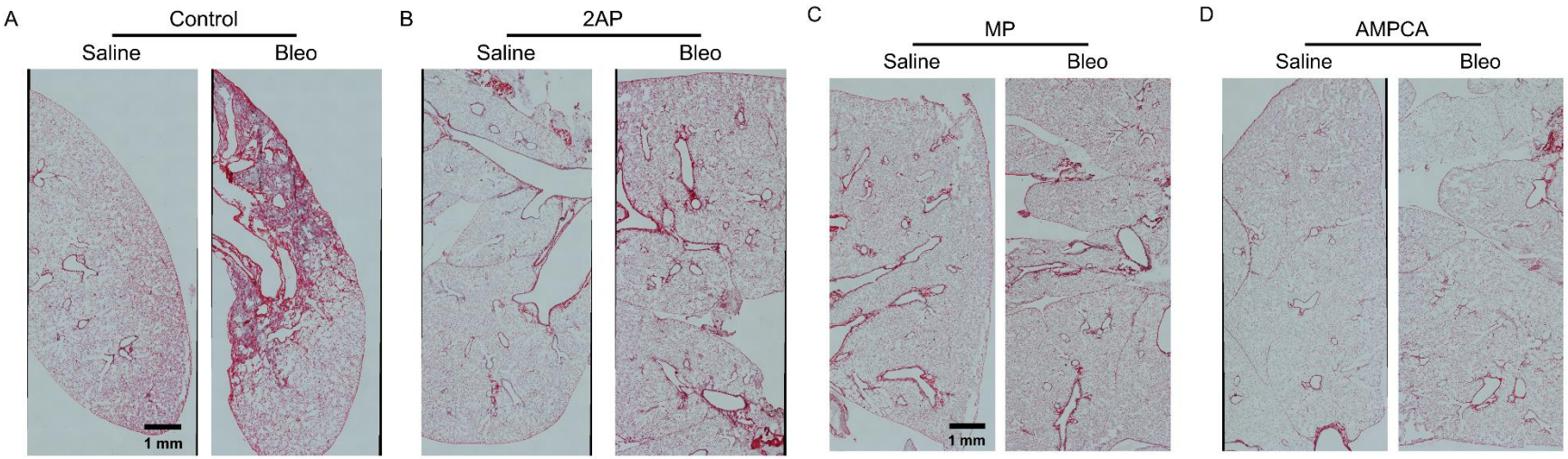

Supplementary Figure 10 Picrosirius red staining of lung cryosections. Representative mosaic images of mouse lung cryosections stained with Sirius red. Images are representative of 3 mice aspirated with saline or bleomycin and injected with (**A**) PBS as control, (**B**) 2-acetyl pyridine (2AP), (**C**) Methyl picolinate (MP), or (**D**) 4-amino-1-methyl-2-piperidine carboxylic acid (AMPCA).